

DEPOSITION AND TESTING OF THIN FILM HYDROGEN SEPARATION
MEMBRANES

A THESIS SUBMITTED TO
GRADUATE SCHOOL OF NATURAL AND APPLIED SCIENCES
OF
MIDDLE EAST TECHNICAL UNIVERSITY

BY

FATİH PİŞKİN

IN PARTIAL FULFILLMENT OF THE REQUIREMENTS
FOR
THE DEGREE OF MASTER OF SCIENCE
IN
METALLURGICAL AND MATERIALS ENGINEERING

FEBRUARY 2013

Approval of the thesis:

**DEPOSITION AND TESTING OF THIN FILM HYDROGEN SEPARATION
MEMBRANES**

submitted by **FATİH PIŞKIN** in partial fulfillment of the requirements for the degree of **Master of Science in Metallurgical and Materials Engineering, Middle East Technical University** by

Prof. Dr. Canan Özgen
Dean, Graduate School of **Natural and Applied Sciences**

Prof. Dr. C. Hakan Gür
Head of Department, **Metallurgical and Materials Engineering**

Prof. Dr. Tayfur Öztürk
Supervisor, **Metallurgical and Materials Engineering Dept., METU**

Examining Committee Members:

Prof. Dr. M. Kadri Aydınol
Metallurgical and Materials Engineering Dept., METU

Prof. Dr. Tayfur Öztürk
Metallurgical and Materials Engineering Dept., METU

Assoc. Prof. Dr. H. Emrah Ünalın
Metallurgical and Materials Engineering Dept., METU

Assist. Prof. Dr. Y. Eren Kalay
Metallurgical and Materials Engineering Dept., METU

Assist. Prof. Dr. Hasan Akyıldız
Metallurgical and Materials Engineering Dept., Selçuk University

Date:

11.02.2013

I hereby declare that all information in this document has been obtained and presented in accordance with academic rules and ethical conduct. I also declare that, as required by these rules and conduct, I have fully cited and referenced all material and results that are not original to this work.

Name, Last Name : FATİH, PİŞKİN

Signature :

ABSTRACT

DEPOSITION AND TESTING OF THIN FILM HYDROGEN SEPARATION MEMBRANES

Pişkin, Fatih

M.Sc., Department of Metallurgical and Materials Engineering
Supervisor: Prof. Dr. Tayfur Öztürk

February 2013, 53 pages

Industrial production of hydrogen from the syngas, generated from steam reformation of natural gas or coal gasification, sets conditions for hydrogen separation membranes in terms of operating conditions. An alternative source for hydrogen is a syngas generated by gasification of municipal solid wastes which are likely to set more stringent conditions for the separation membranes. There is therefore, a growing demand for separation membranes with improved permeability and particularly of low cost. Among various alternatives, metallic membranes are particularly attractive due to their high selectivity and permeability for hydrogen, exemplified by palladium (Pd). However, due to high cost of Pd there is still a demand to develop alternative metallic membranes that are of low cost and have improved durability. Efforts have therefore concentrated on either alloying Pd so as to reduce its cost or on alternative membrane compositions of particularly b.c.c. structure.

The current study deals with hydrogen separation membranes and aims to develop infrastructure for rapid identification of membrane compositions with improved permeability. The study is made up of three parts; i) development of sputter deposition system that would allow deposition of multiple compositions in a single experiment, ii) development of substrate material that would support the thin film membranes and would allow permeability measurement and iii) development of a set-up to measure the permeability of the thin film membranes.

In the present thesis, a sputter deposition system incorporating three targets was successfully constructed. The system as tested with palladium-niobium-titanium (Pd-Nb-Ti) ternary system after necessary adjustment would yield thin films of homogenous thickness ($\leq 7\%$) over a sample area of ≈ 150 mm diameter. A total of 21 substrates each in 19 mm diameter arranged in triangular form in the substrate holder could successfully be deposited where composition distributions covered a greater portion of Pd-Nb-Ti ternary phase diagram. The structure of the deposited thin films can successfully be controlled by substrate temperature as well as by the pressure of plasma gas (argon). With the help of these parameters, structural diversity can also be produced beside the compositional variation.

As for substrates, two materials were investigated. These were titanium dioxide (TiO_2) modified porous stainless steel (PSS) and anodic porous alumina (AAO). TiO_2 modified PSS due to its associated surface roughness leads to the deposition of films with defected structure which as a result is not gas tight. AAO produced via anodization of aluminum foil had a regular (40-60 nm) pore structure that provides a suitable surface for thin film depositions which could be defect free. However, AAO is very delicate and fragile which makes it difficult to adapt it as a support material for permeability measurement/hydrogen separation purposes.

Finally, a set-up was developed for measurement of hydrogen permeability which is capable of measurement over a wide pressure and temperature conditions, i.e. hydrogen pressures up to 10 bar and temperature as high as 450 °C.

It is recommended that so as to identify compositions with improved permeability, Nb or a similar metal which has extremely high permeability could be used as a support material. This would tolerate the evaluation of the films which are not totally defect free.

Keywords: Hydrogen Separation Membrane; Thin Film Deposition; Permeability Measurement; Anodized Alumina; Pd-Nb-Ti.

ÖZ

İNCE FİLM HİDROJEN AYIRICI MEMBRANLARIN ÜRETİMİ VE TEST EDİLMESİ

Pişkin, Fatih

Yüksek Lisans, Metalurji ve Malzeme Mühendisliği Bölümü
Tez Yöneticisi: Prof. Dr. Tayfur Öztürk

Şubat 2013, 53 sayfa

Hidrojenin endüstriyel olarak buhar reformasyonu ya da kömür gazlaştırma yöntemleriyle elde edilen sentetik gazlardan üretilmesi, ayırıcı membranlar için zorlu bir uygulama alanıdır. Alternatif bir kaynak olarak kentsel atıkların gazlaştırılması ile üretilen gazlar ise hidrojen ayırıcı membranlar için daha da zorlu koşullar oluşturmaktadır. Bu nedenle özellikle düşük maliyetli ve üstün geçirgenliğe sahip ayırıcı membranlara olan ihtiyaç giderek artmaktadır. Birçok alternatif arasında, metalik membranlar özellikle yüksek hidrojen seçicilikleri ve üstün hidrojen geçirgenlikleri nedeniyle ilgi çekicidir, örneğin Pd ince filmler bu konuda yaygın olarak kullanılmaktadır. Bununla birlikte Pd nin yüksek maliyeti nedeniyle, düşük maliyetli ve üstün dayanıklılığa sahip alternatif metalik membranların geliştirilmesine halen ihtiyaç duyulmaktadır. Bu nedenle hem Pd nin alaşımlandırılarak maliyetinin düşürülmesi hem de özellikle b.c.c. yapıya sahip alternatif membran kompozisyonlarının geliştirilmesi araştırma çabalarının yoğunlaştığı alanlardır.

Bu çalışma, hidrojen ayırıcı membranlarda yüksek geçirgenliğe sahip membran kompozisyonlarının hızlı bir şekilde saptanmasını amaç edinmektedir. Çalışma üç kısımdan oluşmaktadır; i) tek deneyde çoklu kompozisyonların saçırma ile çöktürülmesine imkan sağlayacak kaplama sisteminin geliştirilmesi, ii) ince film membranları destekleyecek ve geçirgenlik ölçümlerine imkan sağlayacak altlık malzemesinin geliştirilmesi ve iii) ince film membranların geçirgenliklerini ölçmeye yönelik bir test düzeneğinin geliştirilmesidir.

Bu tezde, üç hedefli bir saçırma sistemi başarı ile geliştirilmiş ve sistem Pd-Nb-Ti ye uygulanmıştır. Gerekli ayarlamalardan sonra yapılan çöktürme ile Pd-Nb-Ti 150 mm çapında örnek alanında film oluşturmuş ve bu filmde kalınlık homojenliği $\leq 7\%$ olarak sağlanmıştır. Membran geliştirmeye yönelik gerçek deneylerde, 19 mm çapında altlıklar kullanılmış ve bu altlıklar saçırma hedeflerinin hemen üstünde üçgen diziliminde yerleştirilmiştir. Toplam 21 altlık üzerine yapılan çöktürme, Pd-Nb-Ti üçlü faz diyagramının büyük bir kısmını kaplayacak kompozisyon dağılımında oluşturulmuştur. Çöktürülen ince filmlerin yapıları altlık sıcaklığı ve plazma gaz basıncı ile başarılı bir şekilde kontrol edilmiştir. Bu parametreler yardımıyla, oluşturulan ince film membranlarda kompozisyon çeşitliliği yanı sıra yapısal farklılıklar da üretilebilmiştir.

Altlık olarak iki malzeme incelenmiştir. Bunlar TiO_2 ile modifiye edilen gözenekli paslanmaz çelik ve gözenekli alüminadır. TiO_2 ile modifiye edilen gözenekli paslanmaz çeliklerin pürüzlü yüzeyleri, kusurlu yapıların çöktürülmesine neden olmuş ve bu yapılarda gaz sızdırmazlığı sağlanamamıştır. Alüminyum folyodan eloksal işlemiyle üretilen gözenekli alüminalar 40-60 nm lik kanallar içerecek şekilde başarı ile üretilmiştir. Ancak bu şekilde üretilen yapıların çok hassas ve kırılgan olmaları nedeni ile geçirgenlik testi/hidrojen ayırıcı uygulamalarına adapte edilebilmelerinde zorluklar olduğu tespit edilmiştir.

Son olarak, çalışma kapsamında hidrojen geçirgenlik ölçümlerini gerçekleştirmeye yönelik bir düzenek geliştirilmiştir. Geliştirilen düzenek 10 bar'a kadar hidrojen yüklemesine ve 450 °C ye kadar sıcaklıklarda test yapılmasına olanak vermektedir.

Bu çalışmanın amaçları açısından altlık konusunda yaşanan zorlukların, üstün geçirgenliğe sahip metalik altlıkların kullanılması ile aşılabileceği düşünülmektedir. Bu açıdan metaller içerisinde en üstün geçirgenliğe sahip Nb' nin uygun bir altlık adayı olabileceği sonucuna varılmıştır.

Anahtar kelimeler: Hidrojen Ayırıcı Membran; İnce Film Çöktürme; Geçirgenlik Ölçümü; Anodize Alüminyum Membran; Pd-Nb-Ti.

*Dedicated to my beloved Berke Öksüz
and
my family*

ACKNOWLEDGEMENTS

I would like to express my gratitude to my supervisor, Prof. Dr. Tayfur Öztürk for his guidance, advice, support, encouragement and valuable suggestions throughout the course of the studies. It has always been a privilege to work with such a special person.

I would also like to express my gratitude to Assist. Prof. Dr. Hasan Akyıldız for his encouragement and valuable suggestions throughout the course of the studies.

Thanks are to all my friends at the Department of Metallurgical and Materials Engineering, METU, especially Hakan Yavaş, Burak Aktekin, Alptekin Aydın, Yusuf Yıldırım, Arif Atalay Özdemir, Cemal Yanardağ and Necmi Avcı for their support in the completion of the thesis. Thanks are also to Serkan Yılmaz for his patience and support during SEM studies.

I would also like to acknowledge Department of Physics, METU for thickness measurements in this study.

I would like to thank my parents for all the love, trust, support, worries and encouragement. Their great influence made me who I am today.

Finally, very special thanks to Berke Öksüz, for her endless love, encouragement, patience, advices and support during my thesis studies.

This study was supported by The Scientific and Technological Research Council of Turkey (TÜBİTAK) Grant No: 109M580.

TABLE OF CONTENTS

ABSTRACT.....	iv
ÖZ.....	vi
ACKNOWLEDGEMENTS.....	ix
TABLE OF CONTENTS.....	x
LIST OF TABLES.....	xii
LIST OF FIGURES.....	xiii
CHAPTERS	
1. INTRODUCTION.....	1
2. LITERATURE REVIEW.....	3
2.1. Hydrocarbon-based Hydrogen Production.....	3
2.2. Hydrogen Purification Methods.....	4
2.2.1. Dense Metallic Membranes.....	6
2.2.1.1. Pd and Pd based f.c.c. membranes.....	9
2.2.1.2. B.c.c. based membranes.....	12
2.2.1.3. Amorphous membranes.....	13
2.3. Porous Substrates for Hydrogen Separation Membranes.....	14
2.4. Production of Separation Membranes.....	16
2.4.1. Rolling into Sheet/Foil.....	16
2.4.2. Electroplating.....	16
2.4.3. Electroless Plating.....	17
2.4.4. Spray Pyrolysis.....	18
2.4.5. Chemical Vapor Deposition.....	18
2.4.6. Magnetron Sputtering.....	18
3. EXPERIMENTAL PROCEDURES.....	21
3.1. Magnetron Sputtering System.....	21
3.2. Sputter Deposition of Thin Films.....	22
3.3. Substrate Fabrication.....	23
3.4. Permeability Measurement.....	23
3.5. Material Characterization.....	25
4. RESULTS AND DISCUSSION.....	27
4.1. Deposition of Thin Film Membranes.....	27
4.1.1. Deposition of Thin Films with Compositional Variation.....	27
4.1.2. Structural Control in Deposited Films.....	30
4.2. The Preparation of Substrate for Hydrogen Separation Membranes.....	34
4.2.1. Porous Stainless Steel.....	34
4.2.2. Anodization of Aluminum.....	36
4.3. Permeability Measurements.....	37
4.3.1. TiO ₂ Modified PSS Substrate.....	37
4.3.2. AAO Substrate.....	40

4.4. Discussion.....	42
5. CONCLUSIONS AND RECOMMENDATION FOR FUTURE WORK.....	45
REFERENCES.....	46

LIST OF TABLES

TABLES

Table 2.1. Hydrogen permeability of selected membranes.....	9
Table 2.2. Effect of alloying elements in H ₂ permeability of Pd membranes. The permeability values are normalized with that of pure Pd.....	11
Table 2.3. Thermal expansion coefficient of selected materials.....	15
Table 4.1. EDS analysis of thin films deposited on substrates arranged in triangular form...	29

LIST OF FIGURES

FIGURES

Figure 2.1. Different transport mechanisms in porous membranes (Basile and Gallucci 2011)....	5
Figure 2.2. Schematic representation of H ₂ permeating through the metallic membranes.....	6
Figure 2.3. Hydrogen permeability of selected pure metals.....	8
Figure 2.4. Pd-H binary phase diagram (Gillespie and Galstaun 1936).....	10
Figure 2.5. Pd-H equilibrium isotherms (n= atomic H/Pd) up to 571 K (Wicke and Nernst 1964)	11
Figure 2.6. Schematic representation of thin film membrane supported by a porous substrate.....	14
Figure 3.1. The view of Magnetron sputtering system.....	21
Figure 3.2. Base-plate of a vacuum chamber showing the positions of deposition components...	22
Figure 3.3. (a) Schematic representation of permeability tester and (b) the view of the permeability tester.....	24
Figure 3.4. Schematic representation of the test cell in the permeability tester.....	26
Figure 3.5. The view of the test cell in the permeability tester (left) and graphite gaskets used in sealing the membranes (right).....	26
Figure 4.1. Multiple sample holder design for magnetron sputtering system.....	27
Figure 4.2. The view of plain glass substrate after removal of kapton tape.....	28
Figure 4.3. The view of the chamber during thin film deposition.....	28
Figure 4.4. The distribution of the membrane compositions as mapped in Pd-Nb-Ti ternary system.....	30
Figure 4.5. SEM microstructure of thin films deposited on substrate kept at room temperature (left) and substrate heated to 300 °C (right) a) thin film close to Ti (Membrane 11), b) thin film close to Nb (Membrane 16), c) thin film close to Pd (Membrane 21) and d) thin film at the center of the holder (Membrane 9).....	32
Figure 4.6. XRD patterns of Membrane 9 sputter deposited at RT and 300 °C with plasma gas pressure of 5 mTorr and 10mTorr.....	33
Figure 4.7. Rietveld refinement of XRD pattern of Membrane 9 deposited at 5 mTorr and at 300 °C.....	33
Figure 4.8. The SEM micrographs of 0.1 μm grade porous stainless steel a) the surface b) the cross-section.....	34
Figure 4.9. The surface appearances of PSS filter after Pd-Nb-Ti sputter deposition.....	35
Figure 4.10. The surface SEM micrograph of TiO ₂ modified PSS filter.....	35
Figure 4.11. The stages of two-step anodization; a) first anodization, b) oxide removal, c) nano-pattern formation, d) second anodization, e) removal of aluminum, f) opening of close-ends.....	37
Figure 4.12. The flux rates versus differential argon pressure 0.1 μm PSS (left) and TiO ₂ modified PSS (right).....	38
Figure 4.13. The flux rates versus differential argon pressure for membrane 1, 9, 16, 21 deposited on TiO ₂ modified PSS together with a bare TiO ₂ modified PSS.....	38
Figure 4.14. The SEM micrographs of Pd-Nb-Ti membranes deposited on TiO ₂ modified PSS a) Membrane 1, b) Membrane 16, c) Membrane 21 and d) Membrane 9.....	39
Figure 4.15. H ₂ flux versus pressure difference curves of Membrane 20 at various test temperatures.....	40
Figure 4.16. H ₂ flux versus square root of pressure difference curves of Membrane 20 at various test temperatures.....	41
Figure 4.17. Logarithm of hydrogen permeability versus the inverse of test temperature for Membrane 20. The test temperatures are 310, 350 and 400 °C.....	42

CHAPTER 1

INTRODUCTION

Increasing awareness of deleterious effects of fossil fuels on environment, and their reducing resources, engenders a requirement of new feasible energy source which is as efficient as fossil fuels. Among all possible candidates, hydrogen appears to be best suited energy carrier for that purpose. Hydrogen is vastly available in the universe and has the highest energy content per unit weight compared to any of the known fuels. Unlike fossil fuels, using hydrogen as an energy source produces only water as a byproduct. This could become a solution to issues related to energy security including global climate change and air pollution.

As the most common hydrogen production methods steam reforming of natural gas, coal gasification and biomass processes yield hydrogen as a component in a gas mixture, syngas. Therefore; hydrogen should be separated from the gas mixture to obtain it in pure form. There are several methods to separate H₂ out of syngas; pressure swing adsorption, cryogenic distillation, and separation based on the use of membranes. The latter is divided into two groups; porous and dense membranes. Among these, dense metallic membranes are particularly attractive due to their very high hydrogen selectivity and the relatively high hydrogen permeability. Pd is the most popular separation membrane in this respect. It has high permeability and at the same time has the ability to split H₂ molecule to its atomic form, which is the first stage in hydrogen permeation through the membrane. However, Pd-H system is subject to a phase transformation, the so-called α - β transformation, which embrittles the membrane if not kept away from the critical (temperature-hydrogen pressure) conditions. The embrittlement together with the high-cost of Pd restricts the use of Pd and Pd based membranes in industrial applications. Efforts have therefore concentrated on either reducing the Pd content of the membranes or to find altogether new alternatives which were free of Pd. Alloying Pd with Ag and Cu reduces the cost as well as make the alloy resistant to hydrogen embrittlement. Currently the alloys Pd-Ag membranes are in commercial use.

Pd-free membranes based on b.c.c. structure are particularly attractive. This is due to the fact that metals such as Nb, V and Ta are far superior than f.c.c. Pd with respect to hydrogen permeability. However, b.c.c. membranes also suffer from hydrogen embrittlement due to their very high level of hydrogen solubility in them. The efforts to produce mechanically durable membranes have therefore concentrated on reducing the level of hydrogen solubility while maintaining the high permeability. Attempts to achieve this, involved alloying of b.c.c. metals in binary, ternary and sometimes in multi-component form. Another drawback of b.c.c. membranes is the insufficient catalytic activity at their surfaces. Therefore, it is necessary to coat them with a thin layer of Pd so as to make them catalytically active.

Membranes are produced with a variety of techniques. Most common are electroless plating and thin film depositions. Another approach to reduce the Pd content is to decrease the membrane thicknesses. The reduction in thickness serves two purposes. One is to reduce the amount of Pd used in the membrane and the other is to increase hydrogen permeances since the permeation is inversely proportional to the membrane thickness. However, thinner membranes have relatively lower mechanical strength especially at higher temperatures; therefore thickness reduction has certain limits.

One way to produce thinner membranes while providing efficient mechanical and thermal durability during operation is the deposition of thin films on a porous support material. The purpose is then to deposit a very thin selective layer on a mechanically durable material. The support material needs to

compatible with the membrane both physically and chemically. One of the key properties is thermal expansion compatibility between the membrane and the substrate which can lead to problems under cycling operational conditions. Another requirement is the surface condition of the support material which affects the membrane-substrate adhesion and sets requirements for the minimum film thickness to be deposited on the substrate. The most common support materials are; Vycor glass, Al_2O_3 and stainless steel, all in porous form.

The developing improved membranes via both alloying Pd and finding alternative Pd free compositions are not always successful and require extended coordinated efforts. Therefore traditional approach of synthesizing one membrane composition at a time and testing it for permeability are not always very suitable. A method that would allow the synthesis of multiple material compositions and which may then be evaluated by a rapid screening technique is a highly useful approach to develop new membranes best suited for the purpose.

The present work is undertaken to produce multiple material compositions in the form of thin films and to develop a test procedure to be able to test them for their hydrogen permeability. Membranes were based on Pd-Nb-Ti ternary system. More than 20 compositions were sputter deposited in a single experiment where the substrates formed an array suitably positioned over the sputter sources in a triangular geometry.

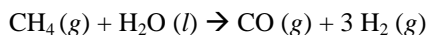
CHAPTER 2

LITERATURE REVIEW

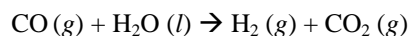
2.1. Hydrocarbon-based Hydrogen Production

Hydrocarbons are the most commonly used raw materials for hydrogen production. One of the leading production methods is steam reforming that uses hydrocarbons such as natural gas, oil, or coal. According to a report published in 2008, the global hydrogen production is 48% from natural gas, 30% from oil 18% from coal and the remaining part is mostly from water electrolysis (Romm 2005). Brief description of these methods is given below.

Steam Methane Reforming provides the least expansive method to produce hydrogen. The process is mainly composed of two steps (Xu and Froment 1989). The first step is reforming of natural gas,



and the second step the water-gas shift reaction;



Equilibrium for the gas-shift reaction favors the products at low reaction temperatures. However, high temperature is required to provide a practical reaction rate. This conflict is solved by the use of two stage shift system. The high temperature water-gas shift reaction yields 73.9% H₂, 17.7% CO₂, 6.9% CH₄, and 1.0% CO whereas low temperature reactions result with 74.1% H₂, 18.5% CO₂, 6.9% CH₄, and 0.1% CO gas mixture (Molburg and Doctor 2003). Additionally, during hydrogen production via steam reforming of methane small amounts of H₂S is normally present in the gas stream.

Coal Gasification process converts the coal into its basic chemical components by reacting with controlled amount of oxygen at high temperatures and pressures. Process yields a gas mixture of H₂, H₂O, CO, CO₂. Gasification process must have further purification step to remove the pollutants from the mixture. The resulting gas generally is composed of 39-41% H₂, 28-30% CO₂, 10-12% CH₄, 18-20% CO plus 0.5-1% H₂S and 0.5-1% NH₃ (Molburg and Doctor 2003). The cost of production is almost twice of that of natural gas due to the ratio of H₂ to C produced (Holladay 2009). In the coal gasification process four different methods are commercially used. These are counter current fixed bed gasifier; co-current fixed bed gasifier; fluidized bed reactor; and entrained flow gasifier (Cortes *et al.* 2009). Currently, gasification process is commonly used for the production of electricity from fossil fuels.

Biomass covers a variety of resources such as agricultural crops, industrial and agricultural wastes. These substances can be used as a feed for hydrogen production by either gasification or pyrolysis processes. The distinction between gasification and pyrolysis is that, gasification requires oxygen during process whereas pyrolysis does not. The method normally involve three steps; pre-treating, heating, scrubbing (cleaning). In pyrolysis process, biomass is transformed to liquid, solid and gas by heating at high temperatures (around 773 K) without the presence of oxygen. Pyrolysis yields hydrogen-rich products which are then steam reformed to produce hydrogen (Holladay 2009 and Kalinci *et al.* 2009). In biomass gasification/pyrolysis, it is important to note that the composition of gas is dependent on the type of resources used and the process temperature. Produced gas composition

generally comprises 30-35% H₂, 15-25% CO₂, 8-12% CH₄, 20-30% CO and 1-3% N₂. Additionally, small amount of H₂S and NH₃ may also be present (Boerrigter and Rauch 2005).

As mentioned above, production of hydrogen from hydrocarbons yields a mixture of various gases such as CO, CO₂, CH₄, H₂O, NH₃ and H₂S. These substances prevent direct usage of produced H₂ gas in PEM fuel cells and other hydrogen related applications. Therefore; separation of H₂ from these gas mixtures has great importance (Pyle 1998, Adhikari and Fernando 2006).

2.2. Hydrogen Purification Methods

There are several purification methods to separate H₂ out of gas mixtures produced through a variety of means. The leading methods are pressure swing adsorption, cryogenic distillation and the separation based on hydrogen selective membranes. The latter method may be in the form of porous membranes or dense metallic membranes. According to Uehara 2002, the choice of the separation methods depends on many factors including H₂ purity, impurity substances, production scale and the cost. A brief description of these methods is given below. Dense metallic membranes are the subject matter of this thesis and are reviewed in greater detail.

In **Pressure swing adsorption** method the gas mixture to be refined is fed through the high surface area adsorbent, typically a zeolite, at relatively high partial pressures (1500-2000 kPa). The working principle in this method is the ability of adsorption of impurity molecules at high partial pressures and subsequently desorption of the impurities at low partial pressures. The undesired gases are adsorbed at surface of the adsorbent while pure H₂ permeates through. During the process, the surface of adsorbent gets saturated by impurity gases. This is why system pressure is decreased to remove the impurities from the adsorbent. So, the process operates on a cyclic basis to provide continuous hydrogen flow.

According to Liu *et al.* 2001, the main advantages of the pressure swing adsorption process are the ability to separate H₂ over a wide range of purities. Depending on the requirement, 99.99 % purity of H₂ can be produced during the life time of the adsorbent (Miller and Stocker 1989). However, due to the nature of working principle, the pressure swing method is effective only over a limited pressure range. The high purity H₂ can be extracted at gas pressures <200 kPa. Thus the pressure is quite low and there is a need for additional post compression processes which increases the cost of operation. The other limitations are that the required scale of operation is quite large and involves an extensive infrastructure. Pressure swing adsorption therefore is applicable for high and medium volume operations and it is impractical for small scale usage and portable operations.

Cryogenic Distillation is a low temperature process. In this process H₂ from the gas mixture are separated using the differences in the boiling points of the feed gas ingredients. The boiling point of H₂ is 20.1 K. This is less than boiling point of all gases except for He (4.1 K). In this method of separation, the level of H₂ purity reached is ~99% by volume (Bernardo *et al.* 2009). Furthermore, process is extremely energy intensive and like the pressure swing adsorption is applicable to a large scale production (Hinchcliffe and Porter 2000).

In purification based on **Hydrogen Separation Membranes** the gas mixture is fed through the sealed selective membrane. Since the membrane only allows permeation of H₂, undesired impurities are rejected. H₂ partial pressure gradient which is the driving force of the process is formed across the permeable barrier. H₂ selective membranes require much less energy in use and are relatively easy to produce and handle. Additionally, membranes can be operated at wide range of temperatures and pressures. Unlike the other methods, separation membranes are feasible to small scale applications. According to Shirasaki *et al.* 2009 another key point of the separation membranes is that they can be used in membrane reactors which allow the H₂ production and purification simultaneously. Depending on the choice of separation membrane, H₂ can be produced with ultra-high purity that cannot be

achieved neither pressure swing adsorption nor cryogenic distillation (Adhikari and Fernando 2006). Separation membranes may be in the form of porous membranes or dense metallic membranes (Ockwig and Nenoff 2007).

Porous Separation Membranes makes use of differences in the molecular size and kinetics of species that make up the gas mixture. Membranes are in the form of nanoporous filters which can be made from a variety of materials such as metals, ceramics and polymers. These membranes can be used at high temperatures and pressures and with gases containing CO and H₂S which are poisonous to metallic membranes. According to Adhikari and Fernando 2006 this type of membranes can exhibit very high permeation rates while hydrogen flux is directly proportional to feed pressure. Due to the nature of porous structure, the membranes are fragile and have limited strength. A limitation of this method is that the purity level that can be achieved is not more than ~99%.

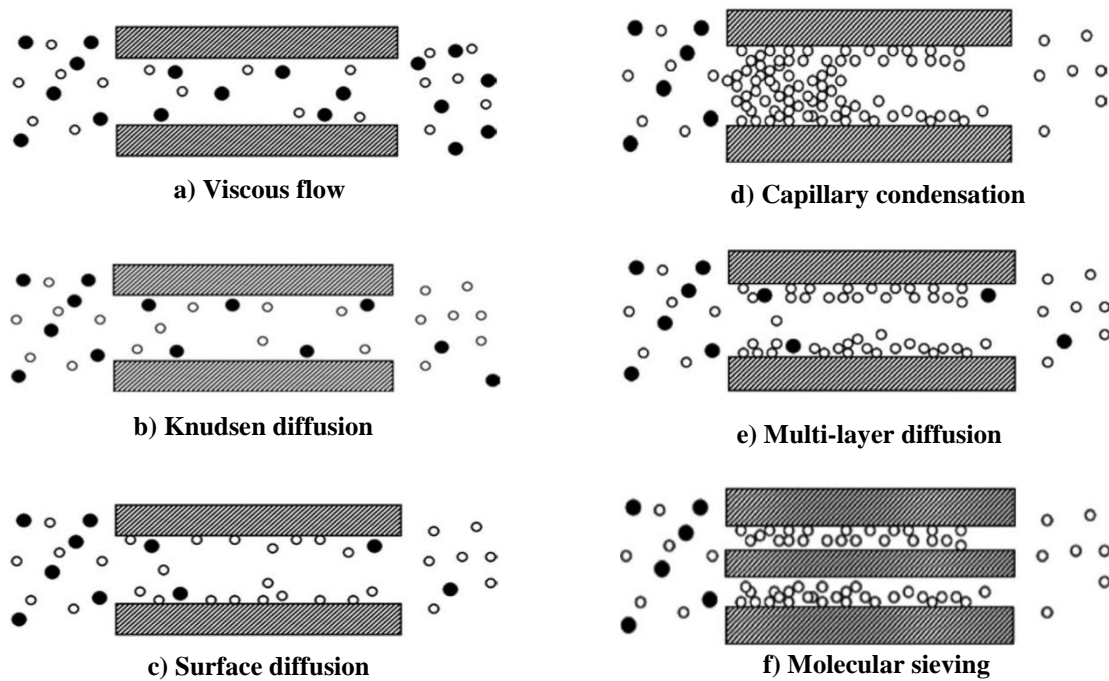


Figure 2.1. Different transport mechanisms in porous membranes (Basile and Gallucci 2011).

Mechanism by which the separation occurs varies depending on the pore size. When the pore size is larger mean free path of the molecules involved, there is no separation, Figure 2.1 (a). For separation to occur the mean free path of the molecules should be comparable to the pore diameter. When the pore diameter is smaller than the mean free path of the gas molecules, molecules collide with the pore wall much more than each other. In such cases separation takes place based on Knudsen diffusion (Saracco and Specchia 1994), Figure 2.1 (b). In the case of one of the gas species is adsorbed by pore wall and diffuses through this adsorption layer is called surface diffusion (Kapoor *et al.* 1989), Figure 2.1 (c). Another alternative is that one of the gas species may condense within the pore due to capillary forces, thus the other species cannot pass through (Lee and Hwang 1986). This kind of diffusion

mechanism is called capillary condensation, Figure 2.1 (d). Another mechanism that would contribute the separation is multi-layer diffusion. This occurs when the surface-molecule interactions are strong so that gas molecules forms multi layers and diffuse over the surface, Figure 2.1(e). In the case of pore size that are smaller than the size of most gas species, only certain molecules in small size can diffuse through the pores which is called molecular sieving, Figure 2.1 (f). The recent work (Ryoo *et al.* 2001) shows that microporous membranes such as carbon molecular sieves provide better separation due to molecular sieving effect.

Separation can also be achieved with the use of dense **Polymeric membranes**. Most of the polymeric membranes are based on polyamide-imide block co-polymers and offer low cost solutions. However, as Miller and Stocker 1989 reported, selectivity levels are poor, especially in the presence of CO₂, H₂O and H₂S due to swelling and compaction. Furthermore, polymeric membranes can be only used in the limited range of temperatures. This limits the usage of polymeric membranes for hydrogen separation processes.

2.2.1. Dense Metallic Membranes

In the case of dense metallic membranes, separation process is quite different as compared to those reported above. The process is based on diffusion of hydrogen in the solid state and normally involves five steps, Figure 2.2.

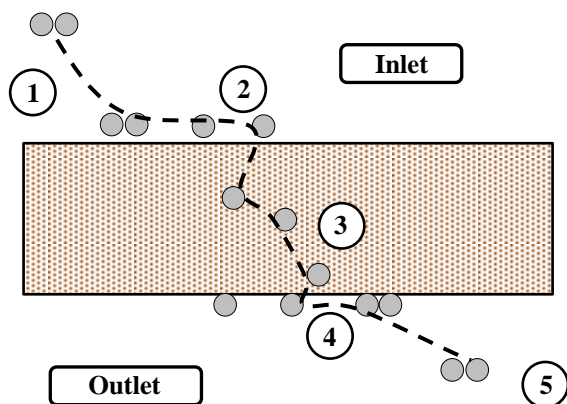


Figure 2.2. Schematic representation of H₂ permeating through the metallic membranes.

The first step is the adsorption of H₂ molecules onto the membrane surface. The second is the dissociation of H₂ molecules to the atomic H on the surface. It is followed by the diffusion of H atoms through the membrane. At the low pressure side the membrane H atoms re-associates into H₂. Lastly, H₂ molecules desorb from the surface. In this process, if the rate limiting step is diffusion of H₂ in the membrane, the H₂ flux is calculated by integration of Fick's First Law.

$$J = -D \frac{dC}{dl} = \frac{D}{l} (C^1_{H_2} - C^2_{H_2})$$

Equation 2.1

Here J is the hydrogen flux ($\text{mol/m}^2\cdot\text{s}$), D is diffusivity of hydrogen in membrane (m^2/s), l is the thickness of the membrane (m), $C^1_{H_2}$ and $C^2_{H_2}$ are the hydrogen concentration at inlet and outlet, respectively (mol/m^3). The concentration of hydrogen is expressed as $C = K\eta$, where K is the hydrogen concentration constant (mol/m^3) and η is the H/Metal atomic ratio. At very low hydrogen concentrations, η is linearly dependent on the square root of partial pressure of hydrogen. Therefore; $P_H^{0.5} = K_S\eta$. Where K_S is the Sievert's constant. Combining the related equations gives;

$$J = \frac{D(K/K_S)}{l} (P^{0.5}_{H_2 \text{ In}} - P^{0.5}_{H_2 \text{ Out}})$$

Equation 2.2

The K/K_S term normally represented by S with a unit of ($\text{mol/m}^3\cdot\text{Pa}^{0.5}$) refers to the hydrogen solubility in the membrane material. In this equation, the product of diffusion coefficient and solubility

$$k = D \cdot S$$

Equation 2.3

is referred to as permeability. The temperature dependence of the permeability of hydrogen through dense membranes can be determined according to the Arrhenius relation (Mardilovich, *et al.*, 1998).

$$k = k_0 \cdot \exp \left[-\frac{E_a}{RT} \right]$$

Equation 2.4

Here R is the universal gas constant ($\text{J/mol}\cdot\text{K}$), T is the temperature (K) and E_a is the activation energy for hydrogen permeation (J/mole). This activation energy can be determined by reorganizing the Arrhenius equation. Taking the logarithm of both sides in equation 2.4;

$$\ln(k) = \left(\frac{-E_a}{RT} \right) + \ln(k_0)$$

Equation 2.5

Thus the plot of $\ln(k)$ versus $1/T$ is a straight line whose slope is equal to $-E_a/R$.

Since the equation 2.2 is based on Sievert's constant, this definition of permeability is valid for low levels of H concentration in the membrane (Sievert's Law is valid up to certain levels of pressure) and for the condition that the rate limiting step in the H_2 permeation is the diffusion through the membrane.

The latter point is quite important since in the case of ultra-thin membranes, the surface processes become more critical than the H_2 diffusion. The same might occur also when the rate of surface reactions are slowed down due to, for instance, by the presence of contaminants in the gas mixture. When the rate limiting step is the surface reactions, equation 2.2 may be written in a more general form. The k/l term in the equation refers the permeance value which is usually used when the thickness of membrane is not precisely known.

$$J = \frac{k}{l} (P^n_{H_2 \text{ Upstream}} - P^n_{H_2 \text{ Downstream}})$$

Equation 2.6

Here the exponent n may take values other than $n=0.5$. The determination of n value would indicate as to which is the rate limiting step. Athayde *et al.* 1994 reported that the exponent approaches a value of $n=1$ in case of 76Pd-24Ag membranes less than $2 \mu\text{m}$ in thickness where the rate limiting step was the

kinetics of surface reactions. Similar thickness values were reported by Jayaraman *et al.* 1995, Nam *et al.* 1999, McCool and Lin 2001. Hurlbert and Konency 1961 had reported that upon exceeding 20 μm , membranes have $n=0.5$ indicating that the diffusion is the rate limiting step.

Ward and Dao 1999 considered all kinetic steps for H_2 permeation emphasized the importance of temperature in H_2 permeation. They claimed that above 573 K, H_2 diffusion is the rate limiting step even in very thin membranes. A similar temperature was reported by McCool *et al.* 2001. The surface reaction becomes rate limiting only with dilute concentration of hydrogen. On the other hand desorption was found to be critical at very low temperatures.

Dense metallic membranes exhibit reasonable H_2 flux over a wide temperature and pressure range. Permeability of some selected pure metals are shown in Figure 2.3. Maximum H_2 flux varies based on metal and/or alloy composition. The membranes generally operate in the range 673-873 K which is quite suitable for separation processes involved in steam reforming of methane. According to Quicker *et al.* 2000, the temperature range mentioned makes it possible syngas production and separation simultaneously with a single unit which is called membrane reactor.

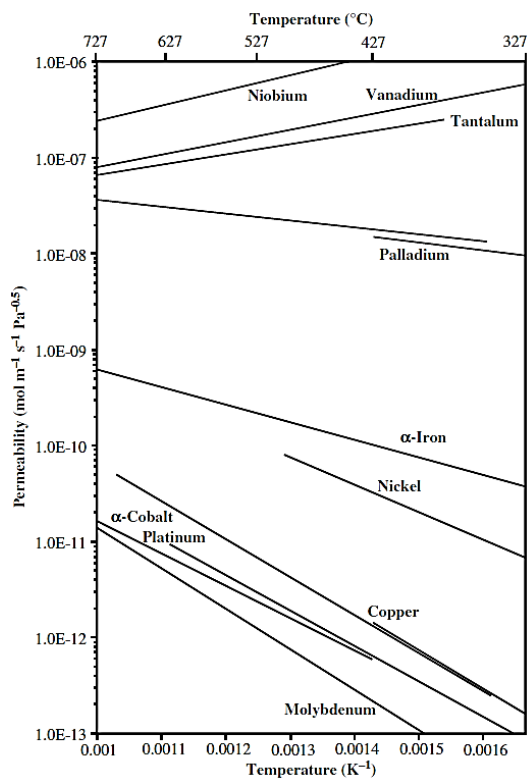


Figure 2.3. Hydrogen permeability of selected pure metals.

Table 2.1. Hydrogen permeability of selected membranes.

Pure Metals	Permeability (mol/m.s.Pa ^{0.5})	Temperature (K)
Nb	1.6×10^{-6}	773
V	1.9×10^{-7}	773
Ta	1.3×10^{-7}	773
Pd	1.9×10^{-8}	773
Metal Alloys		
Pd ₇₇ -Ag ₂₃	3.29×10^{-8}	623
Pd ₄₇ -Cu ₅₃	2.02×10^{-8}	623
Pd ₈₈ -Y ₁₂	7.15×10^{-8}	623
Amorphous Metals		
VCr ₄ Ti ₄	1.3×10^{-8} to 1×10^{-5}	773 - 923
V ₈₅ Ti ₁₅	3.6×10^{-7}	708
Nb ₉₅ Pd ₅	1.3×10^{-7}	573
Nb ₃₉ Ti ₃₁ Ni ₃₀	$0.3 - 2 \times 10^{-8}$	523 - 673
Zr _{36-x} Hf _x Ni ₆₄	$0.6 - 3 \times 10^{-9}$	473 - 673
V _{97.1} Al _{2.9}	$0.7 - 1.8 \times 10^{-9}$	523 - 673

Dense metallic membranes may be classified into several groups; i) Pd and Pd based f.c.c. membranes ii) membranes based on group IVB-VB elements which mostly have b.c.c. structure and iii) membranes that have amorphous structure. Some typical permeability values are given in Table 2.1 (Knapton 1977 and Ockwig and Nenoff 2007).

2.2.1.1. Pd and Pd based f.c.c. membranes

Pd is the most popular metal for hydrogen separation membrane. This is not only due to its high permeability but also due to its catalytic activity in splitting H₂ molecule to its atomic form. Furthermore, Pd is resistant to oxidation (Zhang *et al.* 2009). According to Paglieri and Way 2002 hydrogen purification achieved by Pd membrane, as in other metallic membranes, is extremely high and the impurity level may be expressed as parts per billion (ppb) which might be due to tiny amounts of carbon and other impurities which might diffuse through the metallic lattice and along grain boundaries.

The one of the earliest study on Pd-H system is that by Graham 1866. Pd-H phase diagram as determined by Gillespie and Galstaun 1936 is given in Figure 2.4. Below 293 °C the phase diagram contains three regions; the single α phase (low H solubility phase) region, the single β phase (high H solubility phase) region and a miscible region where both α and β phases are in equilibrium. Both phases have f.c.c. structure but with a different lattice parameter. Figure 2.5 shows Pd-H equilibrium isotherm at various levels of hydrogen pressure. As seen in this diagram, first α phase formed. This is followed by $\alpha+\beta$ region where the pressure remains constant. Upon full conversion to β , the pressure rises again. At a fixed hydrogen content corresponding to $\alpha+\beta$ region, when the metal is cooled from an elevated temperature, initially homogenous alloy is converted into a two phase $\alpha+\beta$ structure which results in a considerable volume expansion. This expansion could be as much as 10% in volume (Makceehan 1923 and Kruger and Gehm 1933).

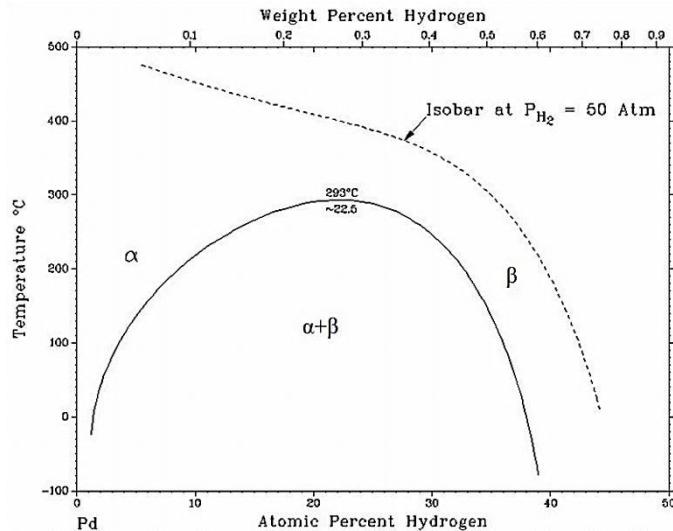


Figure 2.4. Pd-H binary phase diagram (Gillespie and Galstaun 1936).

The volume expansion is the basis for hydrogen embrittlement, a well-known phenomenon in Pd based membranes (Lewis 1967). This phenomenon leads to the formation of micro cracks which severely affects the durability and chemical stability of the membranes.

There are two approaches in handling the embrittlement problem in Pd based membranes. One way is to control the temperature and pressure during operation, so that the membrane is always in one phase region. The other approach is to alloy Pd so that transformation to $\alpha+\beta$ is avoided.

Ag is the most common alloying element to alleviate the membrane embrittlement. In the case of Pd-Ag membranes, Ag in the 10-20 at.% range, the isotherms are comparable to that of the Pd-H system, Figure 2.5, but there is a significant reduction in the critical temperature and pressure.

According to Makrides 1964, the hydrogen solubility at low pressures increases with Ag addition up to 25 at.% and the maximum solubility achieved starts to decrease over 30 at.% Ag addition. Since permeability is the product of diffusivity and solubility, the increase in hydrogen solubility improves the hydrogen permeability of the membrane. Many researchers, Hunter 1960, McKinley 1969, Holleck 1970 and Gryaznov 2000 recommend Ag addition of 20-30 at.% where the permeability of Pd-Ag membranes is up to 1.7-2.0 times of that of the pure Pd.

Cu is another alloying element which can be used for the same purpose. According to Karpova and Tverdovskii 1959, 40 wt.% addition of Cu can reduce the critical transformation temperature below the room temperature. This addition also results in a %10 increase in hydrogen permeability (McKinley 1967). According to Kamakoti and Sholl 2003 this increase in permeability arises mainly from an increase in H₂ diffusivity. An advantage of Pd-Cu membranes is that they are quite resistant to sulfur compounds such as H₂S which is especially important for applications in coal gasification (Gao *et al.* 2004 and Morreale *et al.* 2004).

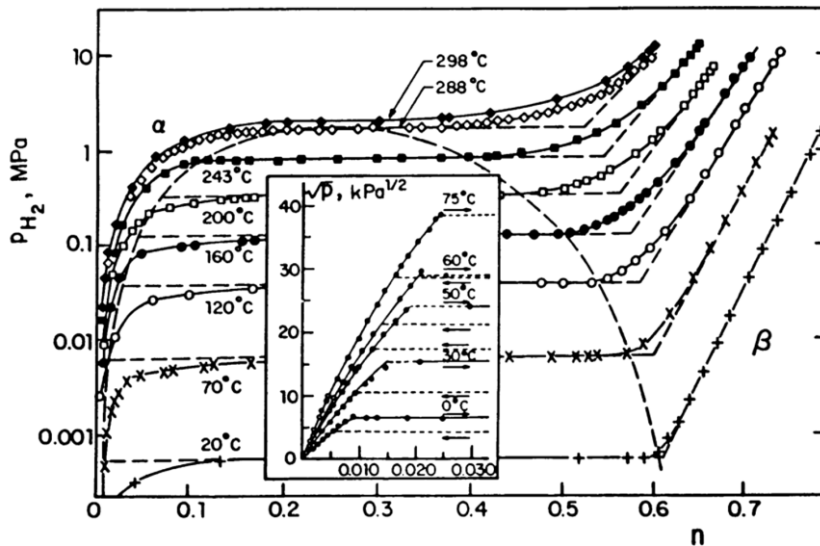


Figure 2.5. Pd-H equilibrium isotherms (n = atomic H/Pd) up to 571 K (Wicke and Nernst 1964).

In addition to Ag and Cu elements such as Y, Fe and Ni could also be used as alloying elements in Pd. The effects of various alloying elements on permeability are summarized in Table 2.2 taken from a review by Gryaznov 2000. Of these, according to Fort *et al.* 1975 Pd-Y is quite comparable to Pd-25%Ag alloy with a higher hydrogen permeability and better durability. Pd-Fe alloy membranes are interesting as they show no phase transformation (Bryden and Ying 2002).

The main drawback of Pd membranes is their high-cost. The efforts to reduce the cost have concentrated either on alloying the Pd to reduce its fraction or to reduce the thickness of the membrane (Keltte and R. Bredesen 2005, Mejdell *et al.* 2009, Pizzi *et al.* 2008). The latter approach is more relevant to production techniques involving thin film deposition, as will be reviewed below.

Table 2.2. Effect of alloying elements in H_2 permeability of Pd membranes. The permeability values are normalized with that of pure Pd.

Alloying element	wt.% for maximum permeability	Normalized Permeability
-		1.0
Y	10	3.8
Ag	23	1.7
Ce	7.7	1.6
Cu	40	1.1
Au	5	1.1
Ru, In	0.5, 0.6	2.8
Ag, Rh	19, 1	2.6
Ag, Ru	30, 2	2.2

2.2.1.2. B.c.c. based membranes

Of the non-Pd membranes, those based on b.c.c. structure are particularly attractive. This is due to the fact that metals such as Nb, V and Ta are far superior than f.c.c. Pd with respect to hydrogen permeability, see Figure 2.3. Therefore b.c.c. metals have been the subject of considerable interest as hydrogen separation membrane. It should be noted that even though b.c.c. metals have relatively high H₂ permeability, they still require a Pd surface layer as a catalytic layer.

Nambu *et al.* 2007 have studied hydrogen permeability in Nb foil membranes. The foils are produced by arc melting in the button-shape ingots and then cold rolled into a foil. The foils 500 μm thick are annealed in high purity argon atmosphere at 1473 K. Finally the foil following argon-ion etching is coated with 200 nm Pd via RF magnetron sputtering. Ductile-to-brittle transition of Nb was determined by in situ punch test apparatus. Buxbaum and Kinney 1996 have examined the possibility of using Nb and Ta heat exchange tubes as separation membranes. The tubes were coated with 1 μm thickness of Pd via electroless plating. The thinnest Ta tube with 70 μm wall thicknesses yielded highest hydrogen permeation of as 0.00147 mol/m² s Pa^{1/2} at 693 K. During the long term test, this flux was reduced by 15% after a month of continuous operation.

Moss *et al.* 1998 studied V and Ta separation membranes in addition to Nb. All membranes were coated with thin layers of Pd film on both surfaces. Prior to Pd deposition, the membranes were ion-milled to remove the native oxide layers at the surface. The membranes were tested at elevated temperatures for durations of up to 775 h and were capable of high rate hydrogen flow but was the subject of embrittlement.

Since hydrogen embrittlement is a general problem in all b.c.c. metals, a number of studies have concentrated on alloying methods that would reduce the embrittlement. Paglieri 2008 investigated more than 250 compositions comprising elements Ti, Ni, V and Nb. In this study, the membranes were produced via arc melting and discs of 0.3-0.5 mm in thicknesses were cut by wire electrode discharge machining. 100 nm thick Pd was coated on both surfaces after the removal of surface oxide layer. Membranes were tested at 973 K and 0.3 MPa for approximately 500 h. Most composition suffered hydrogen embrittlement. This was except for V based alloys which were relatively ductile and exhibited hydrogen permeability comparable to pure Pd.

V-Cu and V-Ti systems were also investigated by Paglieri *et al.* 2005. Among the tested compositions V-5wt.% Ti and V- 10wt.% Cu were the most promising compositions. Paglieri *et al.* 2008 also investigated V-Pd alloys. V-10Pd membrane exhibits hydrogen permeability up to 3.86x10⁻⁸ mol/m.s.Pa^{0.5} at 673 K which is slightly higher than the permeability of Pd-23Ag at the same temperature. The membrane is tested for 1400 h providing stable hydrogen permeability, but it cracked upon cooling at 391 K at the end of testing because of hydrogen embrittlement. Zhang *et al.* 2002 investigated V-Al alloys (0.1-40 at. % Al) which were produced by arc melting in argon atmosphere and then cold rolled into sheets with a thickness of 2 mm. The membranes were embrittled upon testing at 523-673 K, the brittleness increasing when the Al content exceeds 20 at.%. Magnone *et al.* 2012 tested V- 1 at% Y membranes 0.5mm thick in the pressure range of 1.5-3.0 bar up to 673 K under pure H₂, H₂-CO₂ and H₂-CO gas mixtures. The highest hydrogen permeability was reported ~32 mL/min.cm² under pure hydrogen. V-Ni system was studied by Zhang *et al.* 2003 and Dolan *et al.* 2011. In the latter study, some ternary compositions were also investigated of which Ti addition has yielded quite a high permeability.

Ti has normally hexagonal crystal structure, but it could be converted to b.c.c. when deposited in the form of thin films. Thus Kong *et al.* 1992 have produced β-Ti (the b.c.c. allotrope of Ti) using DC magnetron sputtering. The film had higher hydrogen solubility compared to its hexagonal form.

Moreover Ti-13V-11Cr-3Al (wt.%) alloy studied by Hill 1984 had a b.c.c. structure and had a permeability value that exceeds that of unalloyed Pd in the range of 573-698 K.

Yukawa *et al.* 2008 studied Nb-5 mol %X (X = Ru and W) alloys which were arc-melted in a purified argon atmosphere. According to authors the alloys possessed excellent hydrogen permeability and showed no hydrogen embrittlement when used under appropriate permeation conditions, i.e. temperature and hydrogen pressures. They further stated that the addition of Ru or W into Nb improves the hydrogen diffusion at high temperatures. Awakura *et al.* 2011 produced membranes in the Nb-W-Mo ternary system via arc melting and cold rolling. Membranes were 0.5 mm thick. According to authors the addition of Mo into Nb-W alloy reduces the hydrogen solubility in the alloy which brings up improvements in hydrogen embrittlement.

Aoki and co-workers 2005, 2006 and 2012 have studied Nb rich Nb-Ti-Ni and Nb-Ti-Co ternary alloys. With the addition of Ni or Co, the alloys have eutectic two-phase structure. Nb-Ti-Ni system is composed of primary phase b.c.c.-(Nb, Ti) solid solution and the eutectic phase {b.c.c.-(Nb, Ti) + B2-TiNi}, whereas Nb-Ti-Co consist of Nb-rich primary phase (Nb, Ti) and the eutectic phase {TiCo + (Nb, Ti)}. In these systems, the major b.c.c. phase contributes to improved permeability and the remaining phase is claimed to contribute to reduced embrittlement. Nb₅₆Ti₂₃Ni₂₁ composition yielded a hydrogen permeability of 3.47×10^{-8} mol/m.s.Pa^{0.5} at 673 K which is quite remarkable in this alloy group. Highest permeability reported for Nb-Ti-Co ternary alloys occurred in the composition Nb₆₀Ti₂₁Co₁₉ which had a value of 3.99×10^{-8} mol/m.s.Pa^{0.5} at same temperature. This value was 2.6 times higher than that of pure Pd.

Membranes which are produced by arc melting and cold rolling are relatively thick. Thinner membranes can be produced by other techniques such as thin film deposition. Xiong *et al.* 2010 have used magnetron sputtering to deposit thin membranes with Nb₄₀Ti₃₀Ni₃₀, composition. The membranes were deposited under high purity argon atmosphere at 4.5 mTorr for 60 min, at temperatures of 298, 573 and 773 K. The membranes deposited at 298 K were then annealed at 973 K for 30 min in vacuum condition. They have found that the H₂ flux of 6-12 μ m Pd/Nb₄₀Ti₃₀Ni₃₀/Pd/PNS support composite membranes exhibited excellent permeation capability and are several times greater than self-supported Nb₄₀Ti₃₀Ni₃₀ and Pd alloys.

Since b.c.c. membranes have intrinsically higher permeability, attempts have been made to make use of Pd alloys in b.c.c. form. Howard *et al.* 2004 have studied Pd-Cu system and found that the alloys had a b.c.c. structure with Cu in 40-47% range. They reported when the b.c.c. alloys heated up to temperature above 833-863 K in the respective order transforms to f.c.c. structure with a drastic reduction in its permeability. Moreover, once the structure transformed to f.c.c., none of the alloys completely regained the high hydrogen permeability by cooling the alloys down to b.c.c. region.

2.2.1.3. Amorphous membranes

Amorphous materials usually have a more open structure than their crystalline equivalent. Therefore they are expected to have increased hydrogen solubility and thus better hydrogen permeability (Gapontsev and Kondratev 2003). This group of membranes can basically be produced by melting the alloy of desired composition followed by rapid cooling processes such as melt-spinning. The alloys of this group are commonly made up of multi-component alloys based on V, Nb, Ta or Zr which already have high H₂ permeability in their elemental form (Steward 1983).

Evard *et al.* 2001 studied Fe-based (77.4 Fe, 1.1 Ni, 7.7 Si, 13.6 B, 0.2 C) alloys in both amorphous and the crystalline form. Membranes were in the form of foil discs with 15 mm diameter and 25 μ m thick. They have used membranes in as-produced form (without coating with Pd) and found that the surface condition inhibited the adsorption and desorption of H₂, and thus the alloys did not have

acceptable permeability. Furthermore, they found that the amorphous structure started to crystallize above 573 K for long annealing durations.

Xue *et al.* 2001 prepared Ni-B amorphous membranes via modified electroless plating technique. They produced membranes in the solution mixture of nickel chloride, ethylenediamine, potassium borohydride, potassium hydroxide and cadmium sulfate with vigorous stirring. Membranes deposited on commercial α -Al₂O₃ tubes were amorphous with a permeation value of up to 1.0×10^{-4} m³/m².s at 580 K. However the H₂/Ar separation factor had a value of 20 which was quite low.

Dolan *et al.* 2009 produced Ni₆₀Nb_{40-x}Zr_x amorphous alloys via combined melting methods. Firstly, Ni based alloys arc melted and they were then induction melted in argon atmosphere and ejected on to a rotating Cu-Be wheel. Amorphous ribbons were produced in the dimensions of 30 mm wide and 50 μ m in thickness. They found that membranes had permeability values 6 times lower than common Pd membranes at 698 K. Furthermore, they stated the membranes start to crystallize over 773 K.

Yamaura *et al.* 2004 studied ternary Ni-Nb-Zr alloys modified with additional elements such as Al, Co, Cu, P, Pd, Si, Sn, Ta and Ti. Alloy ingots were prepared via arc-melting and then ribbons were produced by a single-roller melt-spinning method in argon atmosphere. Prior to permeability test membranes were coated with Pd layer by sputtering. They found that the additional elements X= Si, Sn, Ta or Ti in (Ni_{0.6}-Nb_{0.4})₄₅-Zr₅₀X₅ lead to amorphous membranes that were subject to severe hydrogen embrittlement. Alloys with X= Al, Co, Cu, P or Pd, on the other hand, were both ductile and had a hydrogen permeability in the range of 1.36 - 2.46×10^{-8} mol/m.s.Pa^{0.5} at 673 K. They concluded that amorphous alloys with Co or Cu have high potential as hydrogen separation membrane.

The metastable nature of amorphous alloys poses some difficulties. According to Zander *et al.* 1999 amorphous membranes exhibit exothermic enthalpies of H₂ absorption; therefore there is a risk of crystallization, decomposition or local changes near the absorption sites. Thus, as reported by Liu *et al.* 2004, most of the amorphous membranes have a tendency to crystallize when operated at temperatures over 773 K the precise value depending on the composition and the duration of use. These restrict the usage of amorphous separation membranes and limit them to reduced temperatures.

2.3. Porous Substrates for Hydrogen Separation Membranes

Hydrogen separation membranes are almost always supported by a porous substrate. This is except for sheet membranes that have sufficient strength to support itself. Support materials cover porous metals; porous stainless steel (Nam and Lee 2001, Mardilovich *et al.* 2002, Tong *et al.* 2005), porous nickel, porous ceramics; Al₂O₃, ZrO₂ (Huang *et al.* 1997, O'Brien *et al.* 2001, Tosti *et al.* 2002) and porous glass; Vycor glass (Uemiya *et al.* 1991, Yeung *et al.* 1995, Bryden and Ying 1995).

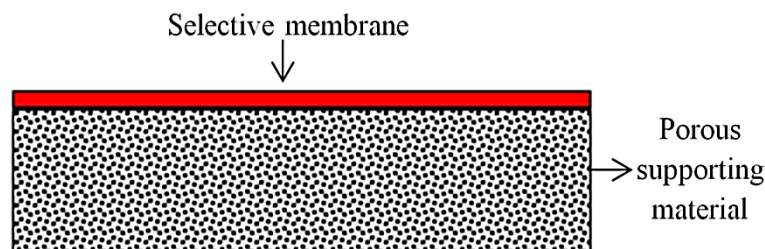


Figure 2.6. Schematic representation of thin film membrane supported by a porous substrate.

One of the important requirements for the support material is its compatibility with membrane. These cover both physical and chemical compatibility. On the physical side, the thermal expansion is an important consideration. The thermal expansion coefficient of commonly used substrates together with Pd, Nb and Ti are given in Table 2.3.

Table 2.3. Thermal expansion coefficient of selected materials.

Material	Thermal expansion coefficient (m/cm.K)
Pd	11.8×10^{-6}
Nb	7.3×10^{-6}
Ti	8.6×10^{-6}
316L stainless steel	16.0×10^{-6}
Ni	13.3×10^{-6}
Al ₂ O ₃	5.5×10^{-6}
ZrO ₂	$8-9 \times 10^{-6}$
Vycor glass	7.5×10^{-7}

Vycor glass is a special type of glass invented by Corning Inc. which is produced via multi-step processes. Firstly, alkali borosilicate glass is typically melted and formed in desired shape. Then a heat treatment is applied to form two distinct phases, one of which is rich in alkali and boron oxide and the other phase is almost pure silica. The alkali and boron oxide phase can be easily dissolved in acid solution. Thus, the remaining body is just silica in porous form. It has the advantage of small and uniform pores typically 4 nm and moreover it is thermally stable at the temperatures where the membranes are used (Bryden and Ying 1995). Vycor based hydrogen separation units were already manufactured by Altinisik *et al.* 2005 and Kuraoka *et al.* 2004. In the latter study, Vycor tube in dimensions of 5 mm diameter and 60 mm in length was coated with a thin Pd film by electroless plating. One end of Vycor tube sealed with nonporous quartz tube by melting. The membranes exhibited 4.9×10^{-8} mol/m².s.Pa hydrogen permeance at 723 K. However, there was a considerable mismatch in thermal expansion coefficient of Vycor with Pd, see Table 2.3. As a result, the Pd experienced cracking under thermal cycling conditions. Additionally, the brittle nature of glass may cause implementation problems in sealing and welding.

Al₂O₃ can be produced with a variety of pore sizes; α -Al₂O₃ 50-500 nm and γ -Al₂O₃ (5-20 nm). O'Brien *et al.* 2001 having used both membranes concluded that γ -Al₂O₃ exhibited better adhesion with Pd than α -Al₂O₃. Furthermore, a gas-tight membrane could only be obtained in the case of γ -Al₂O₃ which emphasized the importance of finer porosity. Tosti *et al.* 2002 have used commercial Al₂O₃ porous tubes and manufactured hydrogen separation unit by depositing Pd on it. They found that the membrane (produced either sputtering or electroless plating) fails under thermal cycling due to the mismatch in thermal expansion coefficient, Table 2.3.

Normally porous alumina supports are produced by controlled pressing and sintering of alumina powders (McCool *et al.* 1999) or via sol-gel processing (Xomeritakis and Lin 1997). An alternative method is to produce the porous structure via anodization of aluminum. Masuda and Fukuda 1995 used a two-step anodization process which yielded a porous alumina with pore sizes of 40-60 nm. They pointed out that the pore size is tunable via selection of solutions and processing conditions. They proposed that the anodic porous alumina (AAO) has a potential as a substrate for thin film depositions

Porous stainless steel (PSS) support is particularly attractive due to closer match of its thermal expansion coefficient with that of Pd based membranes. Mardilovich *et al.* 2002 have studied 0.1, 0.2, and 0.5 μm grade PSS filters in great detail. They found that the maximum pore size increases with increasing grade level. They concluded that the membrane thickness must be at least three times the largest pore size in the substrate surface. Otherwise, defect free, gas-tight membranes could not be produced. They further stated that all PSS supports had quite large pores on their surface and that there is no correlation between the grade level and the surface condition of the filter.

Nam and Lee 2001 developed a method so as to improve the surface condition of PSS support. They dispersed submicron Ni powder on the surface and sintered it under vacuum. The pores on the surface were reduced as a result and the smoothness was improved. Su *et al.* 2005 modified PSS with the use of SiO_2 colloidal suspension. The suspension, composed of 20-100 nm particles, was applied onto PSS by dip coating which was then dried at 573 K. They successfully deposited 2-6 μm thick defect-free Pd membranes by electroless plating. Tong and Matsumura 2004 and Tong *et al.* 2005 have used $\text{Al}(\text{OH})_3$ gel to reduce the surface pore size of PSS tube. Having filled the tube with the gel, they annealed the tube at elevated temperatures. Upon decomposition of $\text{Al}(\text{OH})_3$ fine pores are generated in the surface. Gas-tight thin Pd membrane could be directly deposited on the PSS substrate modified by $\text{Al}(\text{OH})_3$ gel.

2.4. Production of Separation Membranes

Hydrogen separation membranes can be produced with a variety of techniques. These include i) rolling into sheet/foil, ii) electroplating, iii) electroless plating, iv) spray pyrolysis, v) chemical vapor deposition, and vi) magnetron sputtering.

2.4.1. Rolling into Sheet/Foil

One of the earliest production methods for separation membranes is rolling of bulk metal/alloy into a foil form. Typically desired compositions are melted and then cold rolled to the desired thickness. Since rolling is a deformation process, some degree of ductility is a requirement to be able to apply this method. This technique yields membranes which are relatively thick.

Zhang *et al.* 2002 investigated V-Al (0.1, 1.0, 3.0, 10, 20, 30 and 40 at.% Al) alloys which were in the form of foil. They arc melted the alloys into ingots in argon atmosphere, and then the ingots were cold rolled down to a thickness of 2 mm. They found that alloys of V up to 20% Al were sufficiently ductile therefore could successfully be rolled to a foil form. Nambu *et al.* 2007 studied Nb foils as a hydrogen separation membrane. Firstly, the metal were produced by arc melting in button-shape ingots and then cold rolled into foils which were 500 μm thick. Prior to permeation tests, the foils were finally annealed in high purity argon atmosphere at 1473 K.

Membranes which are produced by melting, together with the cold rolling processes, provide bulk self-supporting membranes that are nonporous and dense. However, they are produced in relatively larger thicknesses.

2.4.2. Electroplating

Metal membranes can be electrodeposited on a suitable substrate via electroplating. It takes place in an electrolyte solution which includes one of the solutions of the desired metal. Typically pure Pd can be coated using PdCl_2 precursor in an electrolyte solution. In a recent study, Chen *et al.* 2008 coated 5 μm Pd membrane on a porous stainless steel tube at 323 K via a mixture of PdCl_2 , $(\text{NH}_4)_2\text{SO}_4$ and NH_4OH electrolyte under low current while the tube was rotating. The membrane yielded a reasonable permeability providing H_2/He selectivity over 100,000.

In a similar study Lee *et al.* 2003 produced Pd membrane using Pd(C₃H₅)(C₅H₅) electrolyte. They deposited this on a PSS substrate modified by Ni powders which are then further modified by silica to prevent intermetallic formation. They observed extensive number of pinhole formation and cracks after one month testing at 723 K.

Nam *et al.* 1999 produced dense Pd-Ni alloy membranes on Cu-Ni-PSS composite substrate via a vacuum assisted electrodeposition. The substrates were integrated with a module which allows vacuum to be applied to the opposite side of the substrates during coating. The electroplating was carried out using electrolyte made up of PdCl₂, (NH₄)₂SO₄, NiSO₄.6H₂O and NH₃ and Pt reference electrode. The process yielded a membrane 1 μm thick with the permeances between 16.4-155x10⁻⁶ m²/h.atm in the temperature range of 723-823 K.

In a similar study, Nam and Lee 2001 produced Pd-Cu membrane on porous stainless steel support modified by SiO₂ by vacuum electrodeposition. They used the same solution as above except for NiSO₄.6H₂O which was replaced by copper cyanide (CuCN). The membrane thickness was 2μm and the composition was Pd- 37% Cu by weight. The measured H₂ permeance was 130x10⁻⁶ m²/h.atm and H₂/N₂ selectivity was over 70,000 at 723 K.

Electroplating is an efficient method of forming dense metallic membranes. However, the precursors have complex compositions, and there is insufficient control in the compositions of the membranes to be deposited. Furthermore, it requires a conductive material during deposition which restricts the widespread use of electroplating technique.

2.4.3. Electroless Plating

Electroless plating method is similar to electroplating that involves oxidation-reduction reactions in a plating process. However, electroless plating requires a reducing agent in the bath instead of external electrical power. Comparing the electroplating process, electroless plating has the advantage of the use of nonconductive substrates which widen the choice of support material. Additionally, process can yield uniform depositions even on complex shapes. Prior to electroless plating, supports needs to be activated, i.e. seeded with nuclei of the desired composition.

Mardilovich *et al.* 1998 reported defect-free Pd membranes on porous stainless steel supports by electroless plating. They used a mixture of (PdNH₃)₄Cl₂.H₂O, NH₄OH, N₂H₄ as an electrolyte solution and the deposition temperature was 333 K. Pd membranes were coated in the thickness range of 19-28 μm. They had found the permeance of 8 m³/(m²/h.atm^{0.5}) while H₂/N₂ selectivity was more than 5,000 at 623 K.

Cheng and Yeung 1999 produced Pd-Ag composite membranes on Vycor tubes by electroless plating method. They used (NH₃)₄Pd(NO₃)₂, AgNO₃, NH₄OH and N₂H₄ mixture for electrolyte solution. The deposition was carried on for 60 minutes and resulted with approximately 0.8 μm thick Pd-Ag membrane. Uemiya *et al.* 1991 reported Pd membranes on porous glass by electroless plating method. Pd membranes were coated 13 μm thick and exhibited 15.2 m³/h.atm hydrogen permeation at 773 K. However, they found that H₂/N₂ selectivity dropped dramatically over 573 K due to the crack formation.

Electroless plating offers an economical way for production of separation membranes, even of insulator materials. However it has still insufficient control on thickness and compositions which are quite important especially in thin depositions.

2.4.4. Spray Pyrolysis

Spray pyrolysis is a process that occurs by spraying a solution on a heated surface, where the constituents react to form desired chemical compound. Spraying solution is prepared in the manner that all of the reactants would be volatile other than desired compound at the deposition temperature. The process is utilizable for the deposition of wide range materials (Mooney and Radding 1982). The use of spray pyrolysis in the context of hydrogen separation membrane, however, is not very common. Li *et al.* 1993 produced 1.5-2 μm thick Pd/Ag alloy membrane on porous Al_2O_3 by spray pyrolysis method. They used $\text{Pd}(\text{NO}_3)_2$ and AgNO_3 solutions in the process. The mass fraction of Ag in the membrane at the support surface was as low as 0.04 while the fraction in the spray solution was 0.1-0.4. The H_2/N_2 selectivity of the membrane at 773 K was 24 which was quite low.

2.4.5. Chemical Vapor Deposition

Chemical vapor deposition (CVD) is a deposition process where chemical precursors are delivered in vapor phase to decompose or react to form solid deposit on a heated substrate. CVD is capable of deposition of pure or alloy compounds in a small thicknesses.

Jun and Lee 2000 reported Pd and Pd-Ni membranes on both γ -alumina/ α -alumina and Ni/PSS support materials by metal organic CVD. Depending on the desired composition $\text{Pd}(\text{C}_3\text{H}_5)(\text{C}_5\text{H}_5)$ and/or $\text{Ni}(\text{C}_3\text{H}_5)(\text{C}_5\text{H}_5)$ precursors were fed to the system for decomposition at 303 K. The deposited membranes were 1-2 μm thick and yielded H_2 permeability of $109\text{-}282 \times 10^{-6} \text{ m}^2/\text{h.atm}$ and $82 \times 10^{-6} \text{ m}^2/\text{h.atm}$ for Pd/Ni/PSS and of Pd/ Al_2O_3 membranes, respectively. The values refer to 773 K where the selectivity was 1,600 and 1,000 in the respective order.

Itoh *et al.* 2005 deposited Pd membranes by CVD on tubular Al_2O_3 support which had 0.15 μm average pore size. They used $(\text{CH}_3\text{COO})_2\text{Pd}$ precursor as a Pd source. The decomposition of the precursor has occurred 473-593 K in vacuum environment. The Pd membrane was deposited in the thickness of 2-4 μm which yielded hydrogen permeances up to $102 \text{ m}^3/\text{m}^2\text{h.atm}^{0.5}$ while H_2/N_2 selectivity was 5,000 at 573 K.

CVD process allows highly dense and uniform thin film depositions. However there are several parameters that affect the decomposition chemistry and kinetics such as diffusion rate of precursors, substrate temperature and partial pressure of compounds. It is quite a complicated and costly process not practical for industrial applications.

2.4.6. Magnetron Sputtering

Sputtering process is a member of physical vapor deposition (PVD) techniques. Principally in sputtering, low pressure gas such as argon is fed to the vacuum chamber. Applying high electromagnetic field cause the formation of a numbers of ions and free electrons which is called plasma. Plasma ions are directed and hit the target material where the collisions eject the atoms from target surface which then condense on the substrate surface (Wasa and Hayakawa 1992).

The conventional technology uses direct current (DC) which is referred to as DC sputtering. However, in DC sputtering, the sputtering plasma cannot be sustained over the insulator target due to immediate charge build-up of positive ions on the target surface. For such cases, radio frequency (RF) sputtering could be used (Anderson *et al.* 1962) which discharges the positive ions on the target surface and prevent the charge build-up. Matching network between RF generator and the target is required to optimize the power dissipation in the discharge. Moreover the electrical field of RF in chamber increases the possibility of collision of electrons and molecules. Operating pressure, in this method, can be as low as 1 mTorr.

Magnetron sputtering has some advantages over conventional sputtering technology. Magnetron sputtering system uses strong magnetic fields to concentrate the plasma in front of the target materials that increases the possibility of ion formation and bombardment through the target surface. This is why the deposition can occur at much lower gas pressures and yield higher efficiency compared to the conventional sputtering system. Moreover, magnetic fields also hinder the collision of plasma ions to the substrate material, thus the film quality is improved (Martin 2002).

Furthermore, applying the gas plasma directly onto the substrate, helps clean the substrate surface prior to the deposition. This feature has great importance to obtain high quality thin films. In sputtering, film thickness can be precisely controlled by managing sputtering time, gas pressure and applied power. Moreover, sputtering technique has capability of a precise control the film composition. Since the substrate heating is possible during operation, there is no need for post annealing processes in most applications. Besides the heating option, cooling of the substrate is also possible which widen the control on the structure of the deposited film.

One of the earliest studies on hydrogen separation membrane by sputtering technique is that of Athayde *et al.* 1994. They produced Pd/Ag alloy membranes using 75Pd-25Ag (wt.%) alloy target material. The composition of deposited membrane was the same as the target material. The Pd/Ag alloys in the thickness range of 0.05-0.1 μm were deposited on conventional polymeric gas separation membrane. They have used deposition rates of 75-260 $\text{\AA}/\text{min}$ and found that the best membranes were obtained with high rates. They reported a permeance value of $0.5 \text{ m}^3/\text{m}^2 \cdot \text{h} \cdot \text{atm}$ at room temperature for a 0.05 μm membranes. H_2/CO_2 selectivity was greater than 100.

Jayaraman and Lin 1995 fabricated ultra-thin Pd-Ag membranes (<500 nm) on both $\alpha\text{-Al}_2\text{O}_3$ and sol-gel derived $\gamma\text{-Al}_2\text{O}_3$ substrates. Depositions were carried out in the substrate temperature in a range of RT-873 K. They found two parameters were very critical to the production of gas-tight metal-ceramic composite; surface roughness and the deposition temperature. They claimed that the optimum deposition temperature was 673 K for Pd based membranes. Xomeritakis and Lin 1997 deposited 0.1-1.5 μm thick Pd-Ag membranes on mesoporous $\gamma\text{-Al}_2\text{O}_3$ with 75Pd-25Ag (wt.%) alloy target. The depositions were performed at 5 mTorr argon pressure and the DC plasma power was in the range of 10-60 W. They found that increasing DC power resulted with increasing grain size and higher Pd/Ag ratio in the deposited film. Depositions were carried out at various temperatures so as to understand the effect of deposition temperature. They found that 673 K was the optimum temperature; the lower temperature producing films which were less dense and the higher temperatures producing thermal stresses in the film. The selectivity of H_2/He was in the range of 20-80 whereas the maximum permeation was $1\text{-}2 \times 10^{-7} \text{ mol}/\text{m}^2 \cdot \text{s} \cdot \text{Pa}$.

McCool and Lin 2001 produced Pd-Ag membrane on porous $\gamma\text{-Al}_2\text{O}_3$ by DC sputtering. Target alloy was 75Pd-25Ag (wt.%) and the distance to the substrate was 10 cm. Depositions were carried out at 673 K with 5 mTorr argon pressure. The DC power was applied in the range 10-60 W. Membranes were in the thickness range 600-900 nm. They exhibited good H_2/He selectivity with a value up to 4,000, at 573 K. They found that the hydrogen selectivity improved with the membranes which had been deposited at higher DC power.

Tong *et al.* 2005 synthesized 200-1000 nm Pd-Ag alloy membranes on silicon microsieve supports via DC magnetron sputtering. They used pure Pd and Ag targets. Prior to experiment, deposition rates of pure elements were determined by separate depositions. Depositions were carried out at 7.5 mTorr argon pressure and 135 W and 26 W applied power for Pd and Ag targets respectively which are selected to yield a membrane with a composition of Pd-23 wt.% Ag. The membranes produced however had the composition of Pd-21-22wt.% Ag. They exhibited up to $4 \text{ mol H}_2/\text{m}^2 \cdot \text{s}$ hydrogen flux while the H_2/He selectivity was over 1,500.

Ryi *et al.* 2006 and Kim *et al.* 2008 have sputter deposited 4 μm thick Pd-Cu-Ni ternary alloy membranes. The substrate was a porous nickel. First, they deposited first Pd and then Cu both performed at 1 mTorr argon pressure and 673 K. Subsequent to sputter deposition, the membrane was vacuum annealed at 923 K for 2 hours. This step, called copper re-flow, enables the formation of the membrane with the composition Pd:Cu:Ni 89:4.5:6.5. It was found that the membranes had infinite selectivity regarding N_2 gas tightness due to their pinhole-free structure. Additionally, Pd-Cu-Ni membrane exhibited stable behavior during long term permeability test under cyclic operational conditions (temperature and pressure). The permeance rate as reported by Ryi *et al.* 2006 was 2.3×10^{-7} $\text{mol/m}^2 \cdot \text{s} \cdot \text{Pa}$ at 773 K. Xiong *et al.* 2010 studied another example of ternary system Nb-Ti-Ni as a separation membrane. They successfully deposited 6-12 μm $\text{Nb}_{40}\text{Ti}_{30}\text{Ni}_{30}$ on Ni support at 5mTorr argon pressure while the substrate temperatures were in the range 298-773 K. They found that the lower deposition temperatures resulted with a large amount of defects in the membrane which was attributed to insufficient diffusion, thus less dense membranes were produced. The depositions yielded both crystalline and amorphous films. Permeability tests showed that the amorphous structure exhibited slightly faster H_2 permeability level than the crystalline ones. They reported a flux of 0.014 $\text{mol/m}^2 \cdot \text{s}$ for 6 μm thick amorphous membrane at 673 K.

CHAPTER 3

EXPERIMENTAL PROCEDURES

This chapter covers three sections. First, a sputter deposition system which was developed in this study was described. Then, procedures used in substrate fabrication are presented. This is followed by a description of a set-up used for permeability measurement.

3.1. Magnetron Sputtering System



Figure 3.1. The view of Magnetron sputtering system.

In this study, a thin film deposition system was used specially designed for the purpose of combinatorial study. A general view of the system is given in Figure 3.1. The system had three sputter guns and three thermal evaporation sources. The system has a vacuum chamber with a volume of 65 lt. All connections are of CF type in the chamber except for sputter targets and the main door. Drawing of vacuum chamber is given in Figure 3.2. The chamber is connected with one rotary and one turbomolecular pump which can provide a base pressure in the range of 1×10^{-7} - 5×10^{-8} Torr.

The system hosts two RF (300 watt) and one DC (600 V, 2A) power supplies. RF sputter guns allow the deposition of insulator materials beside metallic ones. Each sputtering target has individual quartz thickness sensor to measure the corresponding deposition rate with a sensitivity of ± 0.1 Å. The thermal evaporation sources are in-between the sputtering targets connected to power supply each with 1500 watt. The system therefore, allows simultaneous and multilayer depositions.

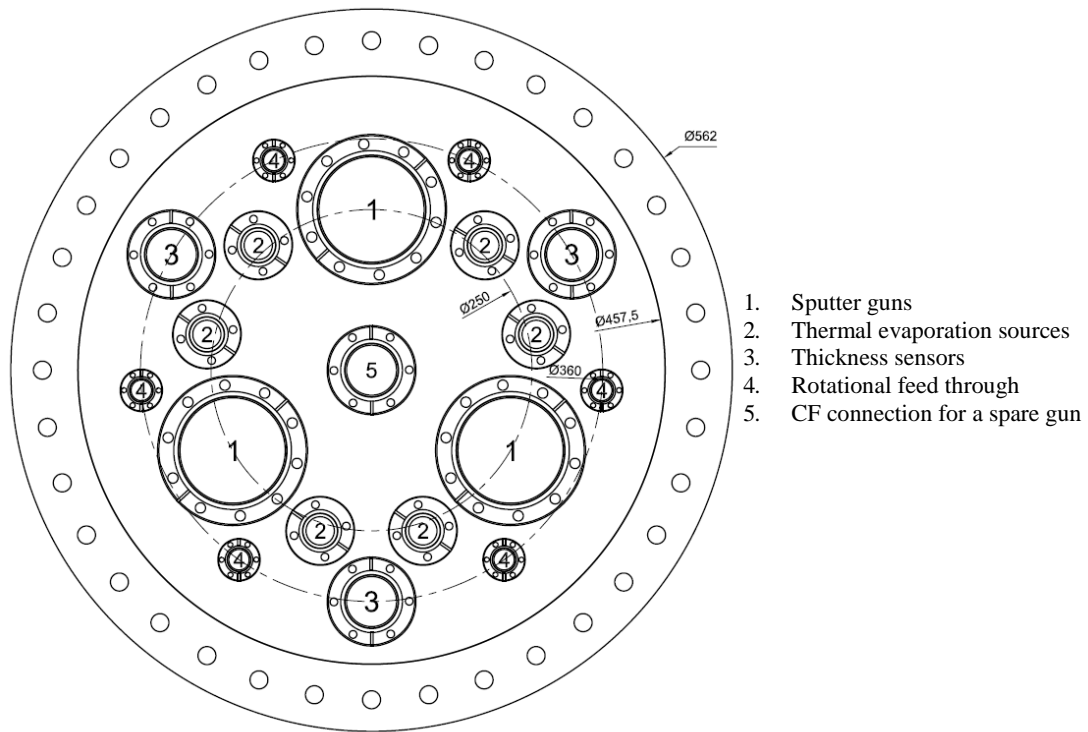


Figure 3.2. Base-plate of a vacuum chamber showing the positions of deposition components.

The substrate holder allows the loading of substrates of up to ≈ 150 mm diameter which can be rotated with 30 rpm. Substrates can be heated up to 300 °C made possible with the infra-red lamps placed above the substrate-holder. In addition to argon, the chamber can be fed with oxygen and nitrogen for reactive sputtering. Each is controlled by individual mass flow controllers that allow rates of up to 50 sccm. The system is connected to a PC which allow the monitoring and control of the operational parameters.

3.2. Sputter Deposition of Thin Films

In thin film depositions, the prepared substrates were placed in the multiple sample holder and then loaded to the substrate-holder. Then, the vacuum pumps were switched on. At the same time, if desired, substrate heating was operated so as to heat the substrates to 300 °C with 5 °C/minute. When the desired vacuum level was satisfied (1×10^{-7} Torr), the chamber was filled with ultra-high purity argon maintained at 10 sccm with a pressure stabilized at a selected value (5 mTorr) by adjusting the gate valve in front of the turbomolecular pump.

Prior to thin film depositions, the individual shutters above the targets were opened and the pre-sputtering was carried out for 10 minutes for the surface cleaning of target metals. During this operation, the main-shutter just below the substrate holder was kept closed. Sputtering targets were palladium (Pd, 99.95%), titanium (Ti, 99.97-99.98 %) and niobium (Nb, 99.95%) targets all in 50 mm diameter (Kurt J. Lesker Co.) Following the pre-sputtering, the main shutter was also opened and the co-sputtering deposition was initiated. Deposition rates were 2 Å/s for all targets. So as to achieve the same deposition rate, the applied powers were 29 W, 120 W RF and 52 W (288 V, 180 mA) for Pd, Ti and Nb targets in the respective order. These values were determined with calibration experiments.

Thin film membranes were produced with a 3 microns thickness. This required a deposition time of 250 minutes. When the desired thickness was attained, all shutters were closed and then the power supplies were turned off. The deposited membranes were cooled down in a controlled manner with a rate of approximately 5°C/min to the room temperature to avoid the thermal stresses.

3.3. Substrate Fabrication

Two types of substrates were used for thin film deposition. These were porous stainless steel (PSS) and anodic aluminum oxide.

Porous Stainless Steel Substrate: Porous support materials used in this study were in the form of discs 19 mm diameter 1 mm in thickness obtained from Mott Corp. Discs were 0.1 µm grade. This value (0.1 µm) refers to the particle retention capability of the filter, i.e. the filter is capable of retaining particles that are larger than 0.1 µm in size.

Anodic aluminum oxide: Anodic porous alumina (AAO) was produced from aluminum foils. The foils used were 150 µm. They were annealed at 500 °C for 4 hours under nitrogen flow. Prior to anodization, samples with a working area of 150 mm² were electropolished at 40 V using in a 1:4 volume mixture of perchloric acid (72 wt.%) and ethanol (98 wt.%) . Electropolishing was carried out <10 °C for a duration of 1 minute.

AAO were produced in a two-step process. In the first step, the anodization was carried out in 0.3 M oxalic acid at a potential of 40 V. Al foil was made anode and the cathode was an aluminum sheet. Following the anodization which was typically carried out for 1 hour, the foil was dipped into a solution maintained at 60 °C made up of a mixture of 6 wt.% phosphoric acid and 1.8 wt.% chromic acid. The purpose of this dipping was to remove the irregular porous oxide layer formed in the surface of the foil. In the second-step having removed the oxide layer, the foil was re-anodized using the same solution and the conditions as in the first anodization. The duration of the second anodization was 15 hours.

The anodization leave a layer 80 micron thick made up porous channels the bottom ends of which are closed by alumina followed by aluminum. The bottom Al layer was removed by electropolishing at 60 V using the same solution as above for 1 minute and the alumina layer which was exposed was removed by dipping the foil into 5 wt.% phosphoric acid solution at 30 °C for 30 minutes.

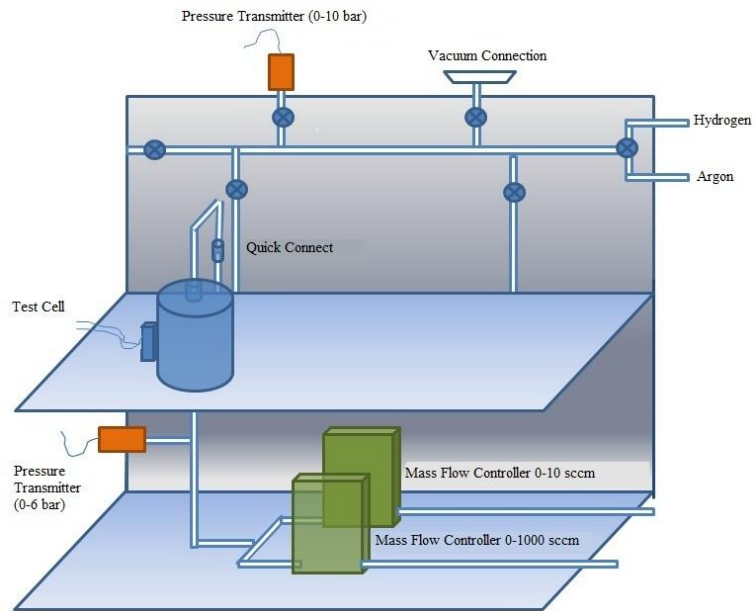
3.4. Permeability Measurement

Permeability is a product of diffusivity and solubility as described in section 2.2.1. This can be measured with the use of equation 2.6, namely;

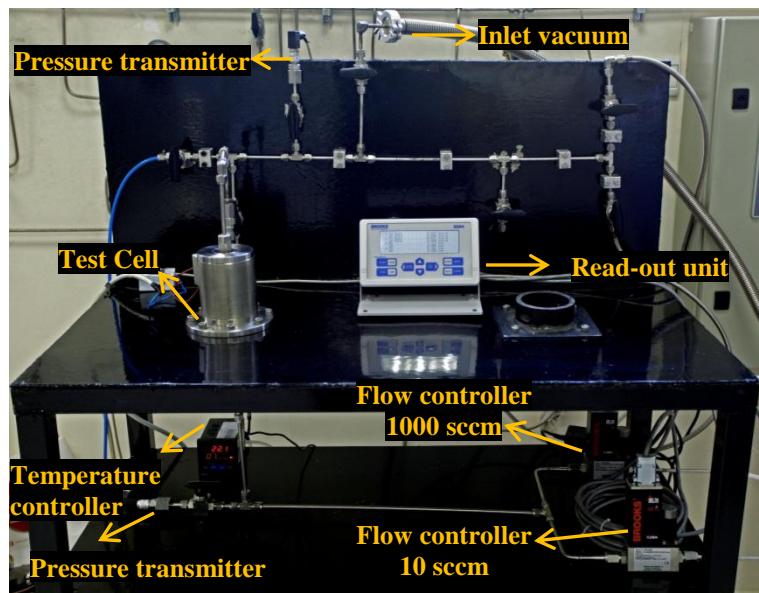
$$J = \frac{k}{l} (P_{in}^n - P_{out}^n)$$

Here k is the permeability, l is the membrane thickness, J is the hydrogen flux and P_{in} and P_{out} are the inlet and outlet hydrogen pressure, respectively. Thus to measure k , for a membrane of known thickness, it is necessary to measure the inlet and outlet pressures and hydrogen flux.

The measurements were carried out in a set-up shown in Figure 3.3. The set-up consist of a test-cell, a gas feeding system at the top and two flow controller/flow meter placed at the outlet at the bottom.



(a)



(b)

Figure 3.3. (a) Schematic representation of permeability tester and (b) the view of the permeability tester.

The test cell comprises a compartment which houses a 19 mm test sample. The cell incorporates a 800 watt heating element which allows the cell to be heated to temperatures up to 450 °C. The temperature of the system is controlled and monitored with ± 0.1 °C sensitivity via a thermocouple located inside the test cell. The schematic representation of test cell is given in Figure 3.4. The sample after testing can easily be removed from the test cell by removing the inlet tubing by a quick connect located at the inlet.

Gas feeding system is connected to a variety of sources; argon, hydrogen or to a vacuum pump. The inlet pressure was monitored by a pressure transmitter (Keller 21Y, 9 bar). Similarly the pressure at the outlet was monitored by a separate pressure transmitter (Keller 21Y, 5 bar). The pressure transmitters in combination simply allow the measurement of the differential pressure between inlet and the outlet.

H₂ flux is monitored by two mass flow meter/controllers (Brooks Instruments SLA5850). The mass flow meters are capable of measurement one in the range of 0-10 sccm and the other in the range 0-1000 sccm. Both pressure transmitters and the mass flow controllers are connected to a four-channel read-out unit (Brooks Instruments, 0254) which can in turn be connected to a PC via RS232 interface.

For testing, the membrane is placed between two CF flanges in the test cell, Figure 3.5 (a). They were made gas tight with the use of two graphite gaskets, Figure 3.5 (b). They were pressed against the sample by driving a hollow nut located above the upper flange.

The membrane was first tested with argon for gas tightness at room temperature. Then, the unit is heated up under argon to the desired temperature. Then argon was evacuated and hydrogen was loaded to the system. The testing for permeability involved hydrogen loadings of up to 10 bar with increments of 0.5 bar. The outlet pressure and the hydrogen flux were then monitored as a function of inlet pressure. Using $n=0.5$, flux is then plotted as a function of square root pressure difference. The slope is k/l , i.e. permeance, from which k is determined. Here if the relationship is not linear this implies the exponent in pressure has a value other than $n=0.5$.

Membranes deposited on both modified PSS and the AAO substrates were tested in the temperature range of 300-400 °C with 50 °C intervals.

3.5. Material Characterization

In the current study, membranes were characterized by X-ray diffraction (XRD) and Scanning electron microscope (SEM). XRD pattern were recorded in Rigaku DMAX2200 using Cu-K α radiation in Bragg-Brentano as well as grazing incidence mode. In the latter the grazing angle was 1°. X-ray data was refined with Rietvelt method using the software Maud (Ferrari and Lutterotti 1994). Structural characterization was carried out using FEI Nova Nano 430. Where necessary elemental analyses were obtained using energy dispersive spectroscopy (EDS) integrated to SEM.

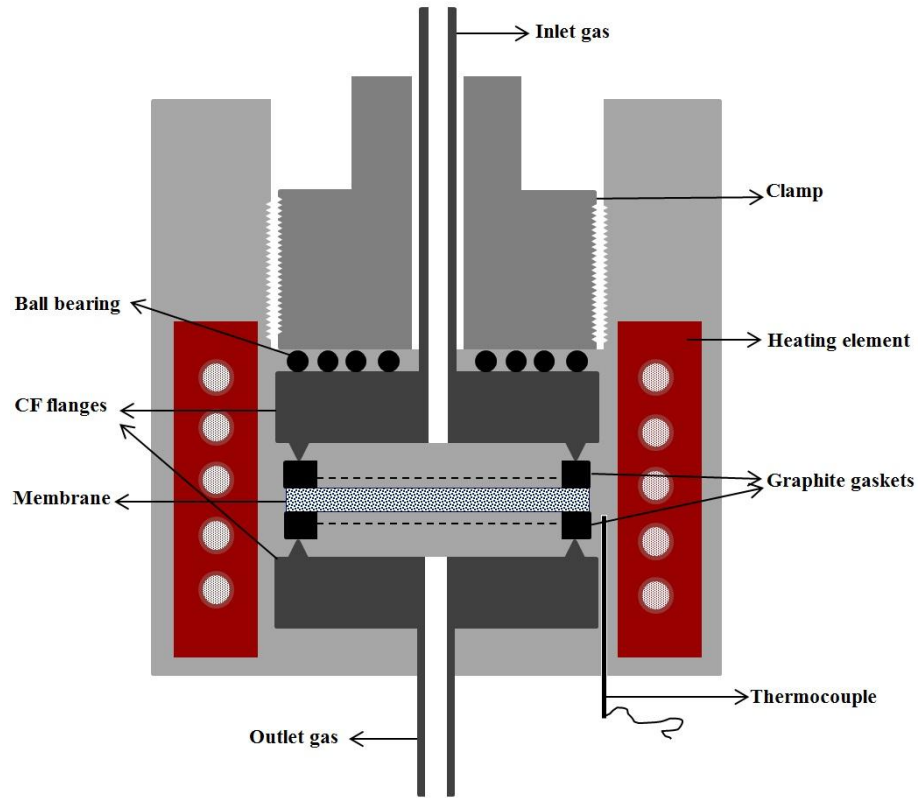


Figure 3.4. Schematic representation of the test cell in the permeability tester.



Figure 3.5. The view of the test cell in the permeability tester (left) and graphite gaskets used in sealing the membranes (right).

CHAPTER 4

RESULTS AND DISCUSSION

The current work on deposition and testing of thin film hydrogen separation membrane involve three parts. The first part deals with the deposition of thin film membranes. This is followed by the preparation of substrate that will support the thin films. The last part deals with testing of thin film-support assembly for permeability.

4.1. Deposition of Thin Film Membranes

4.1.1. Deposition of Thin Films with Compositional Variation

Ternary system selected for the study was Pd, Nb, and Ti. These were obtained as 50 mm sputter targets. So as to obtain compositional variation, a total of 21 samples were prepared. Each sample was 19 mm in diameter arranged in triangular form as depicted in Figure 4.1 (Sample holder is placed just above the targets corners coinciding with the position of Pd, Nb, and Ti targets).

In order to obtain comparable samples, target to substrate holder distance as well as angular positions of the target needs careful alignment so that all samples have the same film thickness. This has been achieved by carefully aligning each target separately. To obtain a uniform thickness, a given sputter target has to yield a deposition rate which is in the ratio of 1:3. The rates referring to the sample in the middle and the sample in the corner close to the target. Regarding three sputter targets, this ratio would result in uniform film thickness throughout the all 21 sample.

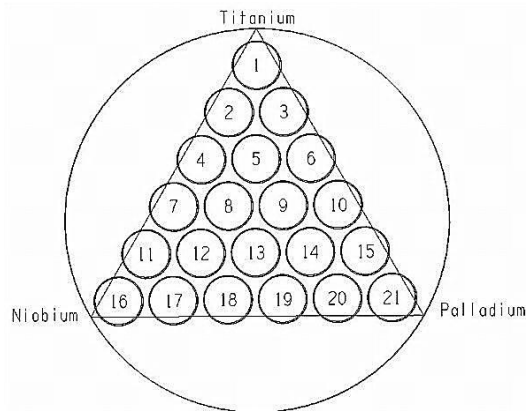


Figure 4.1. Multiple sample holder design for magnetron sputtering system.



Figure 4.2. The view of plain glass substrate after removal of kapton tape.

A series of calibration experiments were, therefore, carried out for each sputter target to adjust its height and the angle so that 1:3 ratio was achieved. For this purpose a 150 mm diameter plain glass was used as a substrate rather than the actual samples.

Prior to depositions, first, the glass was cleaned with acetone for 10 minutes in ultrasonic bath. This is followed by cleaning with methanol and deionized water, each with the same duration. Then, they were dried at 100°C. Following the drying, 6 mm kapton tape was adhered to the glass in a triangular geometry replicating the triangular sample pattern given in Figure 4.1. The glass was then loaded to the substrate holder in the vacuum chamber in the manner that the corners of the triangle align with the each target underneath.

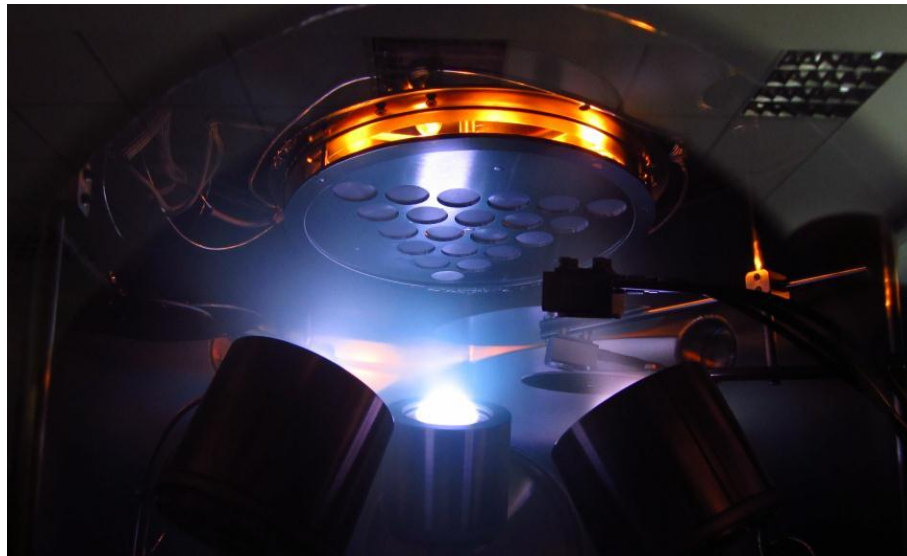
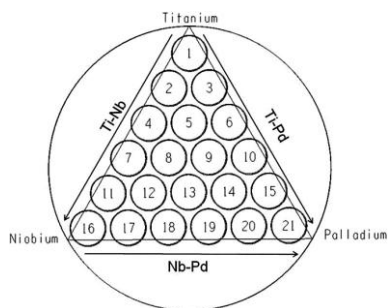


Figure 4.3. The view of the chamber during thin film deposition.

A film was deposited on the glass substrate by activating the single source (normally for duration of 30 minutes), the glass was then removed from the vacuum chamber and the kapton tapes were removed from its surface, Figure 4.2. The thickness values were measured along the traces of the kapton tapes by a profilometer (Veeco, Dektak 6M). The deposition and thickness measurements were repeated in cycles where the height and the angle of the target were adjusted until the desired 1:3 ratio was achieved. The process was repeated for all three targets.

Having aligned the targets, using the power settings given in the experimental section, thin films were deposited on multiple sample holder as given in Figure 4.1. Substrates were 3 mm thick soda-lime glass 19 mm in diameter. All three targets, following a brief pre-sputtering, were activated simultaneously so as to co-deposit films with ternary compositions. A view from the co-sputtering deposition process is given in Figure 4.3.

Table 4.1. EDS analysis of thin films deposited on substrates arranged in triangular form.



2.1Sample	Pd (at.%)	Ti (at.%)	Nb (at.%)
1	13	77	10
2	19	67	14
3	17	66	17
4	19	51	30
5	28	51	21
6	34	51	15
7	20	36	44
8	28	36	36
9	38	38	24
10	48	36	16
11	19	20	61
12	29	27	44
13	41	26	33
14	52	24	24
15	68	20	12
16	13	11	76
17	25	16	59
18	36	18	46
19	57	18	25
20	68	15	17
21	79	10	11

Following the co-sputtering, coated glass substrates were investigated by EDS so as to determine their chemical compositions. The results are given in Table 4.1. These compositions were mapped in the ternary system Pd-Nb-Ti, Figure 4.4. As seen both in Table 4.1 and Figure 4.4, the deposition leads to the production of thin films which cover a considerable portion of compositional space. Thus the system and the sample holder design are quite successful in yielding multiple compositions in a single experiment.

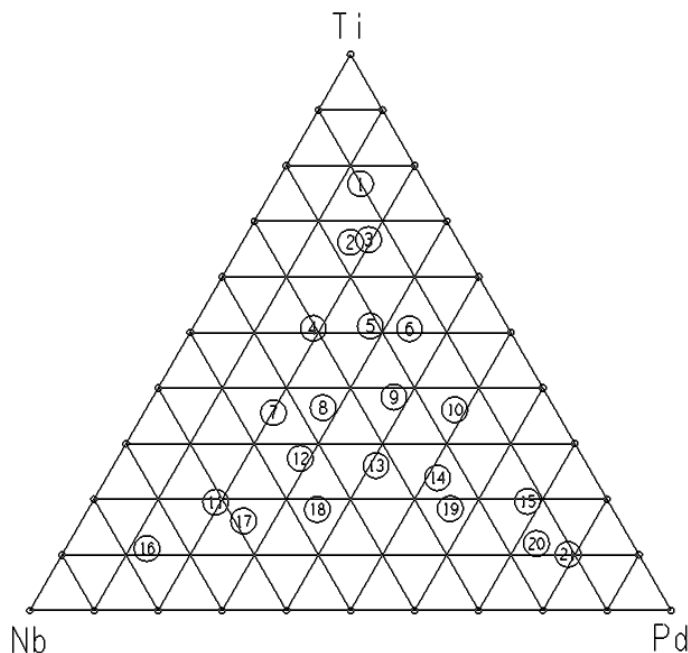


Figure 4.4. The distribution of the membrane compositions as mapped in Pd-Nb-Ti ternary system.

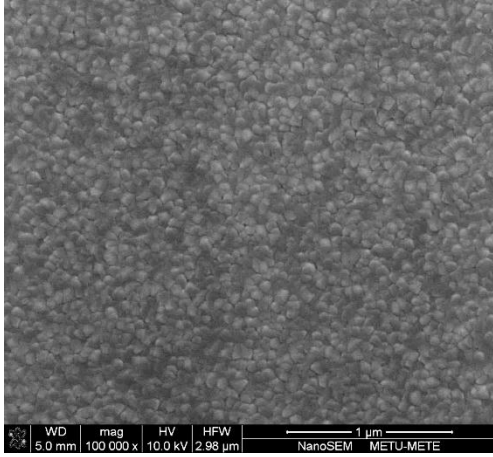
4.1.2. Structural Control in Deposited Films

Yet another aim in the study is to be able to produce thin films with different structures. In order to produce films of different structures, two variables were considered; substrate temperature and the pressure of plasma gas. The depositions were carried out using the same experimental parameters as above.

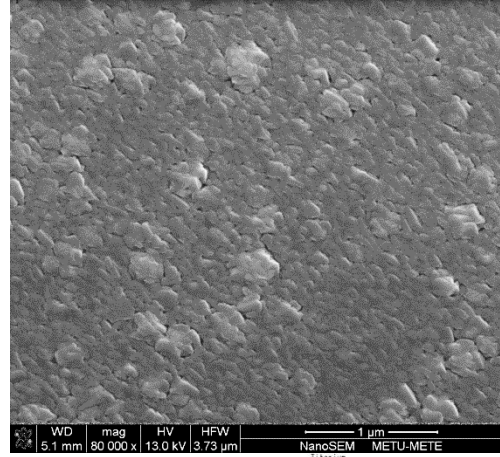
So as to determine the effect of substrate temperature, two experiments were carried out. In one, no heating was applied. In the second, the substrate was heated to 300 °C. It should be pointed out that even without heating, the substrate warms up to a temperature as high as 85 °C.

SEM micrographs of samples from the corners of the sample triangle and the one at the center (Membrane 9) are given in Figure 4.5. It is seen that films deposited without substrate heating has structures which are much finer than those deposited with substrate heating. As an example, thin film close to Ti, deposited without substrate heating, grains are equiaxed roughly 100 nm in size whereas that deposited at 300 °C yields values around 200 nm.

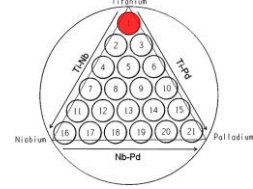
Room temperature



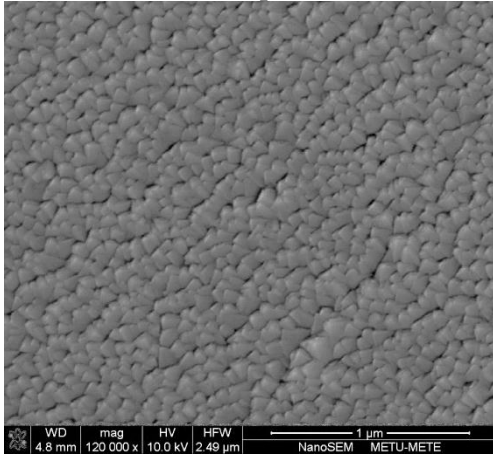
300 °C



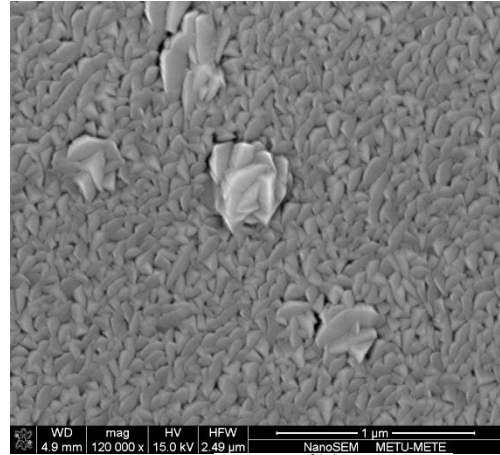
(a)



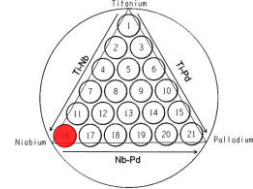
Room temperature

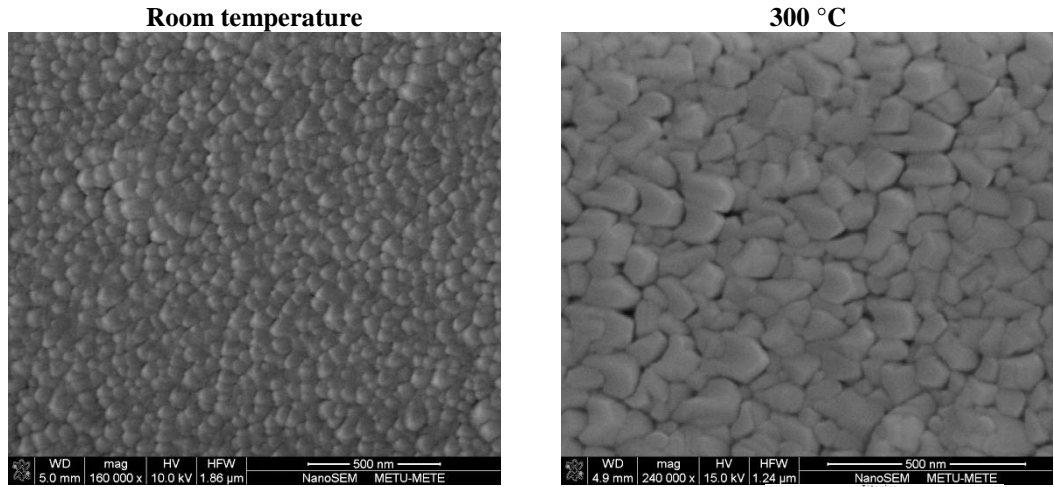


300 °C

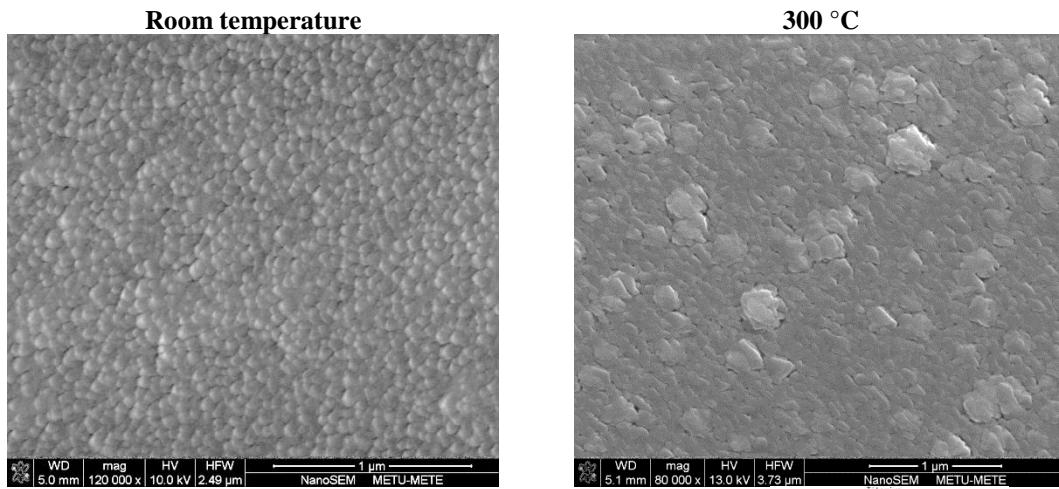
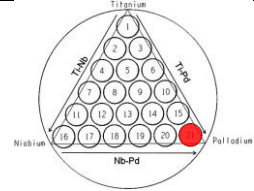


(b)





(c)



(d)

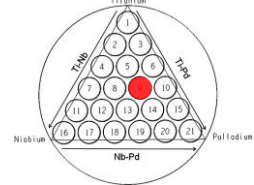


Figure 4.5. SEM microstructure of thin films deposited on substrate kept at room temperature (left) and substrate heated to 300 °C (right) a) thin film close to Ti (Membrane 11), b) thin film close to Nb (Membrane 16), c) thin film close to Pd (Membrane 21) and d) thin film at the center of the holder (Membrane 9).

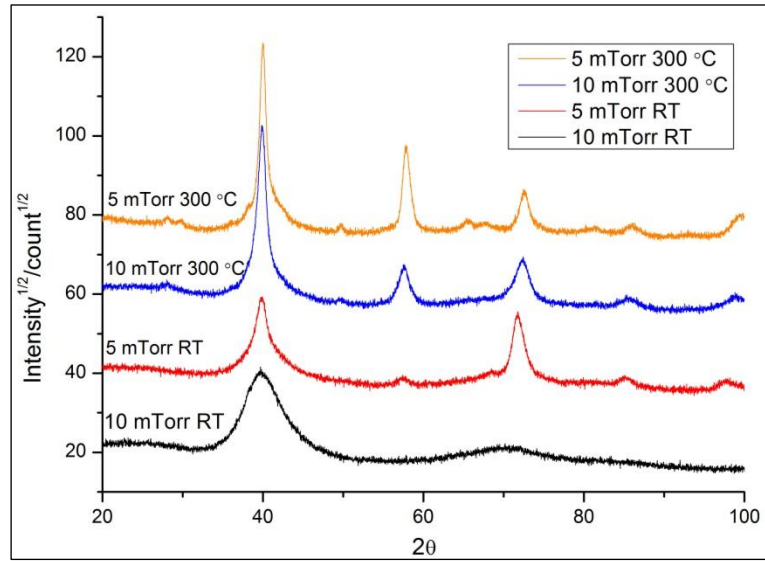


Figure 4.6. XRD patterns of Membrane 9 sputter deposited at RT and 300 °C with plasma gas pressure of 5 mTorr and 10mTorr.

In order to produce thin films with different microstructures, another variable is the pressure of plasma gas. For this purpose, Membrane 9, i.e. membrane in the center of the sample triangle, was selected and the depositions were carried out at 5 mTorr and 10 mTorr argon gas using the plain glass substrates both at room temperature and at 300 °C.

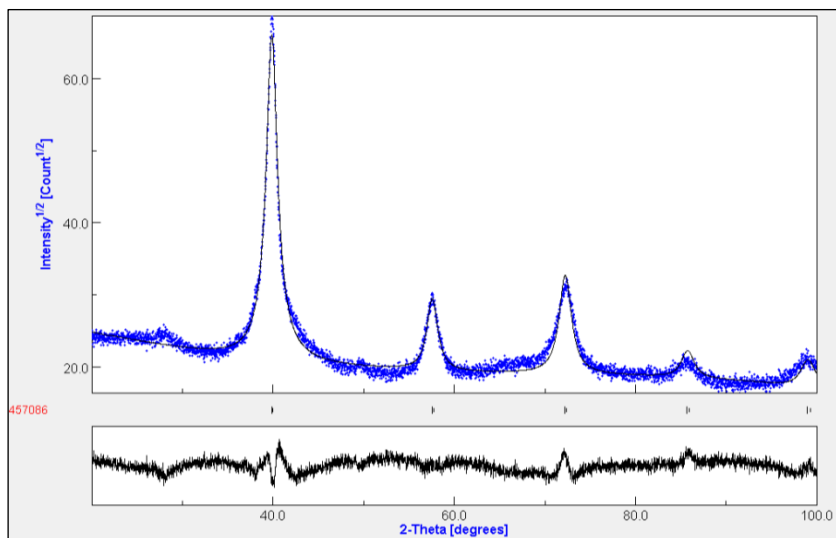


Figure 4.7. Rietveld refinement of XRD pattern of Membrane 9 deposited at 5 mTorr and at 300 °C.

XRD patterns recorded for Membrane 9 in four different conditions are given in Figure 4.6. Patterns were measured with a grazing incidence angle of 1° . As seen in the patterns, the films deposited at 300°C are all crystalline with well-defined peaks in the recorded spectrum. Room temperature deposition especially with 10 mTorr Ar pressure differs substantially from the others as it suppressed the crystallization yielding a membrane with an amorphous structure. The crystalline films given in Figure 4.6, all have b.c.c. structure. The Rietveld refinement of the film deposited at 5 mTorr argon pressure and at 300°C , given Figure 4.7, yields a lattice parameter of $a=3.208 \text{ \AA}$.

4.2. The Preparation of Substrate for Hydrogen Separation Membranes

Thin film membranes require a suitable substrate material for the purpose of supporting the film. Also it is necessary that the support material would allow free passage of gas permeated through the film. For this purpose, two materials were considered; porous stainless steel and anodic porous alumina (AAO).

4.2.1. Porous Stainless Steel

Porous stainless steel substrate was in the form of circular disc filter 19 mm in diameter 1mm thick. The filter was of grade $0.1 \mu\text{m}$. Typical SEM micrographs of PSS are shown in Figure 4.8. Surface micrograph, Figure 4.8 (a), shows the presence of quite large pores. These pores are typically $10\text{-}15 \mu\text{m}$ in size but at places they are as large as $20\text{-}30 \mu\text{m}$.

Figure 4.9 show the substrate after deposition of $3 \mu\text{m}$ thin films at 5 mTorr and substrate temperature 300°C . It is seen that the pores remain as they were and the deposition affected little the overall surface structure of the filter. PSS therefore could not be used as is unless films are made extremely thick. The 3:1 rule as given in section 2.3 requires that so as to ensure the continuity of the film, i.e. without pores, the deposited film has to be 3 times the pore size existing in the surface of the substrate. This implies that for a film thickness of $3\text{-}5 \mu\text{m}$, the largest pore size tolerable in the surface of the substrate is round $1 \mu\text{m}$ or less.

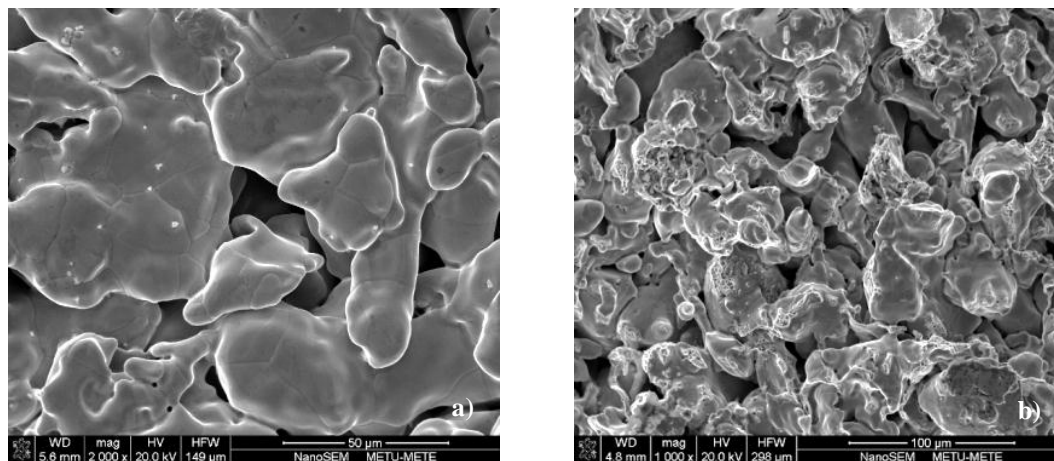


Figure 4.8. The SEM micrographs of $0.1 \mu\text{m}$ grade porous stainless steel a) the surface b) the cross-section.

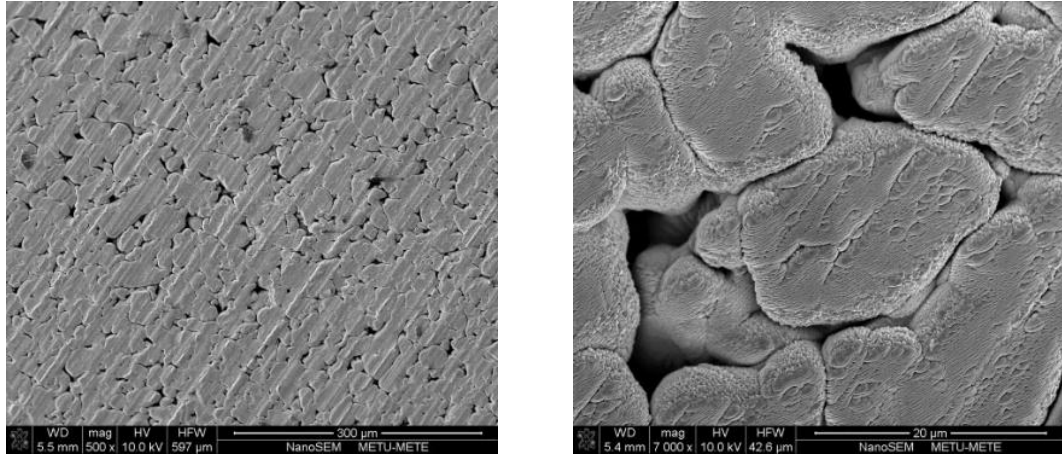


Figure 4.9. The surface appearances of PSS filter after Pd-Nb-Ti sputter deposition.

Thus it is necessary to improve the surface condition of the PSS substrates. A variety of techniques have been used to reduce the surface pores size. These included dip coating as well as spin coating of PSS with fine ceramic powders (TiO_2 , SiO_2), vacuum suction on PSS of $\text{Al}(\text{OH})_3$ and fine powder (TiO_2 , Ni) pressing on PSS. Here only TiO_2 powder pressing will be described.

PSS discs were degreased with Extran (Merck Chem.) and then cleaned with acetone and deionized water. These were carried out in ultrasonic bath for 10 minutes each. Dried PSS discs were then placed into a custom made mould onto which 0.05 g of TiO_2 powder (0.9-1.6 μm , Alfa Aesar) was poured. TiO_2 powder-PSS were pressed in a press with a pressure 250 MPa. Pressed assembly was annealed at 650 $^\circ\text{C}$ for 1 hour. Following the heat treatment, the TiO_2 layer was ground with #3000 and #4000 abrasive papers. A typical example is shown in Figure 4.10. As seen in the figure, TiO_2 powders successfully filled the large pores existing in the surface of the filter. The appearance of TiO_2 layer imply pore sizes which are much less than the value aimed for in this study.

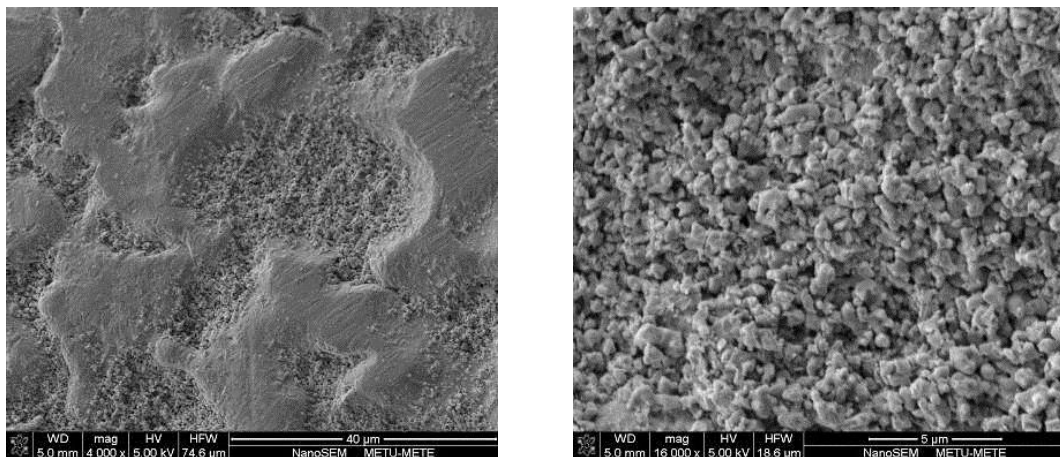
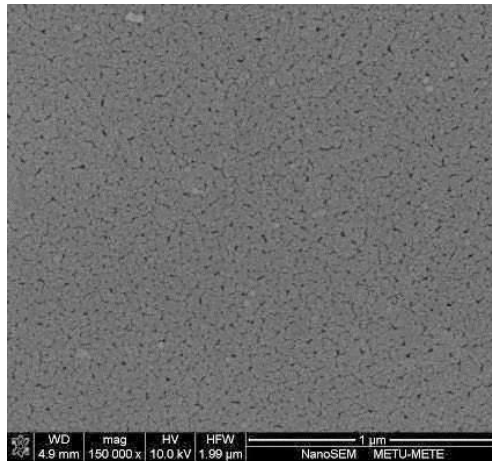


Figure 4.10. The surface SEM micrograph of TiO_2 modified PSS filter.

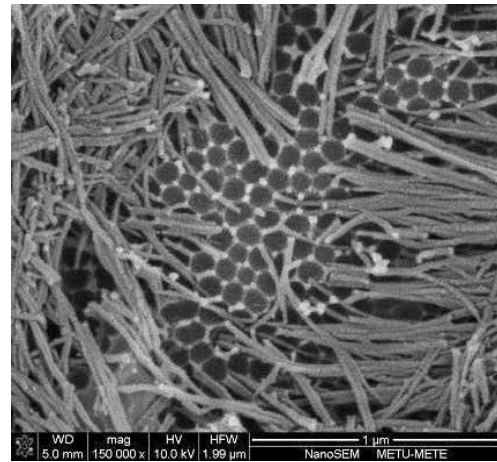
4.2.2. Anodization of Aluminum

The requirement of sub-micron pore sizes in the substrate can easily be achieved by anodization of aluminum. This was achieved by a two-step process. Sequences in the preparation of AAO are given in Figure 4.11. The first step involves the formation of pores of irregular distribution, Figure 4.11 (a). This is then removed by dipping the foil into a solution of phosphoric and chromic acid, Figure 4.11 (b). This leaves out traces of the pores that have been removed, Figure 4.11 (c).

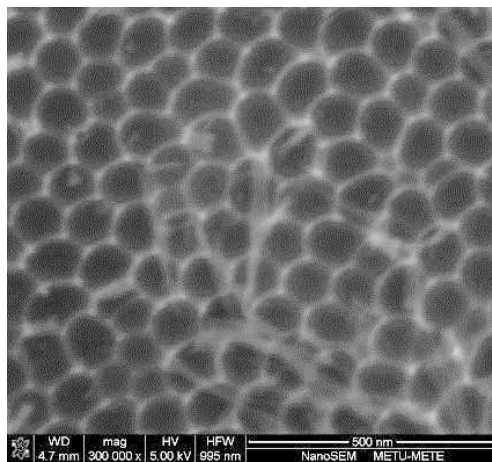
The second anodization follows the regular traces left out in the first step which are in a hexagonal form. At the end of the process, complete ordered pore structure was formed, Figure 4.11 (d). The pores were in the range of 40-60 nm in diameter and they were distributed uniformly throughout the Al_2O_3 structure. The remaining aluminum layer on the other side was removed by electropolishing, Figure 4.11 (e). This was followed by removal of Al_2O_3 layer, at the bottom of the pores, carried out in phosphoric acid. This has yielded a porous Al_2O_3 membrane with pore sizes of 40-60 nm with extremely regular distribution, Figure 4.11 (f).



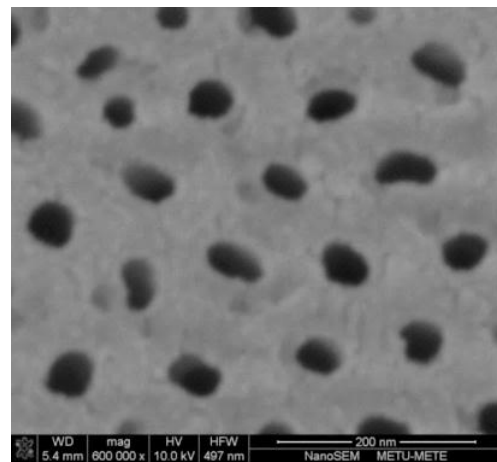
a)



b)



c)



d)

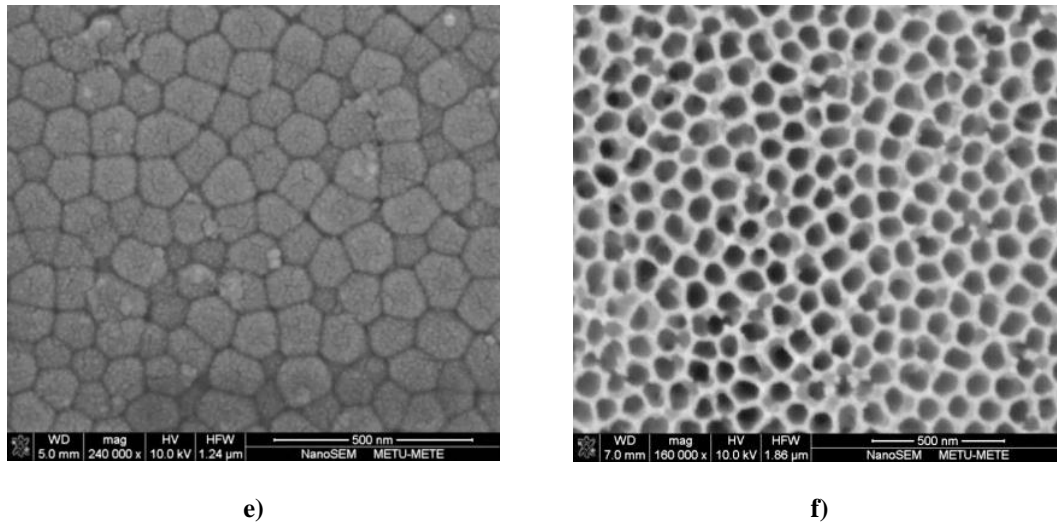


Figure 4.11. The stages of two-step anodization; a) first anodization, b) oxide removal, c) nano-pattern formation, d) second anodization, e) removal of aluminum, f) opening of close-ends.

4.3. Permeability Measurements

Set-up constructed for permeability measurement was tested in two conditions. In one, the substrate was TiO_2 modified PSS and in the other, the substrate was AAO. Membranes which were deposited on the substrate were selected from the sample triangle.

4.3.1. TiO_2 Modified PSS Substrate

PSS substrate was tested as is to determine its initial permeability. Prior to test, the inlet tubing was vacuumed via a turbomolecular pump. Then argon gas was fed to the system up to 3 bar inlet pressure. Then, the flux was measured by the flow meters recorded by a read-out unit. Argon flux determined as a function of pressure difference is given in Figure 4.12 (a). PSS substrate yielded a permeance of $2.54 \times 10^{-5} \text{ mol/m}^2 \cdot \text{s} \cdot \text{Pa}$ for 1 bar inlet pressure.

Similar curve as determined for TiO_2 modified PSS is given in Figure 4.12 (b). This yields a permeance value of $1.49 \times 10^{-6} \text{ mol/m}^2 \cdot \text{s} \cdot \text{Pa}$ for the same condition as above. It is seen that the flux is greatly reduced in modified filter implying considerable reduction in their porosity.

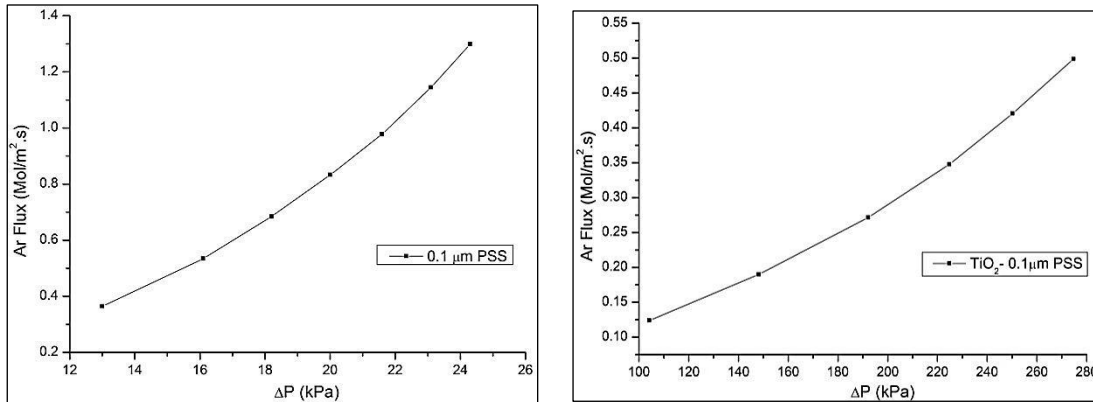


Figure 4.12. The flux rates versus differential argon pressure 0.1 μm PSS (left) and TiO₂ modified PSS (right).

TiO₂ modified PSS substrates were placed in the vacuum chamber and sputter deposited with thin films of various Pd-Nb-Ti compositions. Membranes deposited were 3 μm thick. Coated substrates were subjected to the same test. Flux versus pressure difference curve measured for the samples is given in Figure 4.13. The curve for uncoated TiO₂-PSS is also included in the figure. It should be noted that flux versus pressure values in coated samples are almost the same as the uncoated ones meaning that the coating did not change the permeability of the substrate.

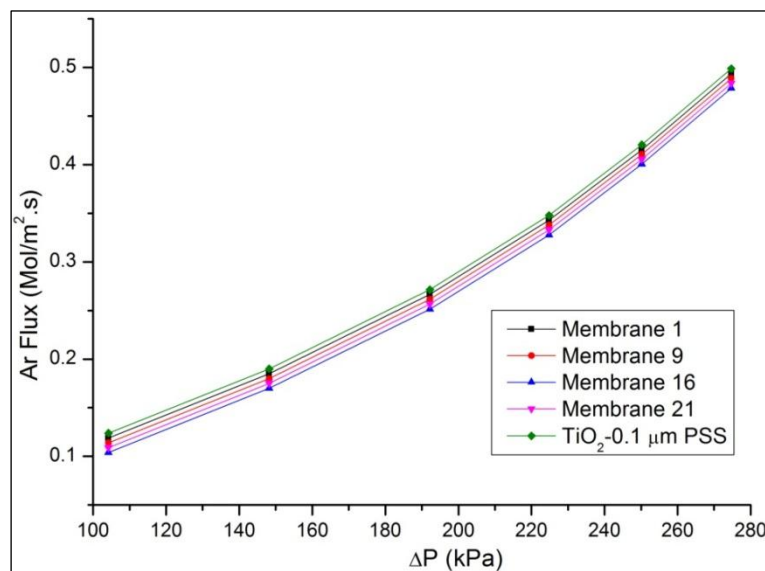


Figure 4.13. The flux rates versus differential argon pressure for membrane 1, 9, 16, 21 deposited on TiO₂ modified PSS together with a bare TiO₂ modified PSS.

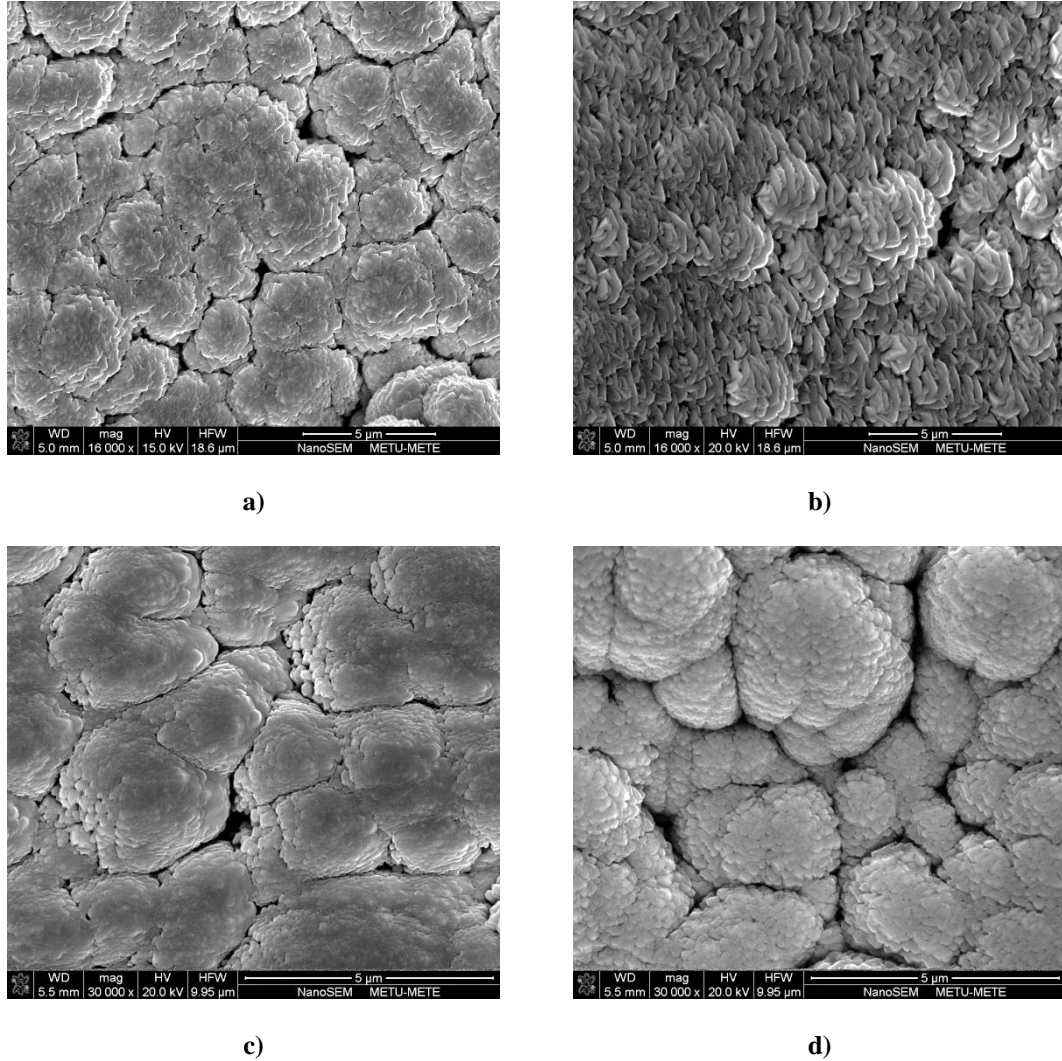


Figure 4.14. The SEM micrographs of Pd-Nb-Ti membranes deposited on TiO₂ modified PSS a) Membrane 1, b) Membrane 16, c) Membrane 21 and d) Membrane 9.

The fact that the deposited TiO₂ modified PSS has the same flux values before and after thin film coating implies that the deposited film is not pore free. Figure 4.14 gives typical micrographs recorded from the coatings on TiO₂ modified PSS.

The morphology is typical of the so-called Zone-I structure as defined by Movchan and Demchishin 1969. Here the deposits have grown to a typical dome structure. Zone-I structure is expected to occur at very low deposition temperatures (i.e. $<0.3 T_m$). Considering that the films had been deposited at 300 °C, the current temperature is indeed within the Zone-I range (Pd $T_m = 1552$ °C, Nb $T_m = 2468$ °C and Ti $T_m = 1660$ °C). The deposited films are therefore expected to have a porous structure since in Zone-I, pores are expected to be present in between the grown islands. Thus the permeability is dictated more by these pores than the film itself. This explains why the flux values were little affected by the deposited film.

4.3.2. AAO Substrate

AAO substrate was tested in bare form, i.e. without thin film coating. Flux versus pressure difference curve is given in Figure 4.15. As compared to PSS, the permeance values, as would be expected, are lower and has a value of 1.38×10^{-5} mol/m².s.Pa for 1 bar inlet pressure (PSS was 2.54×10^{-5} mol/m².s.Pa).

AAO membranes were coated with thin films in the same compositions as before and were first tested at room temperature for gas tightness using Ar. For this purpose, the argon inlet pressure was gradually increased up to 3 bar. No gas flow could be detected with the mass flow meters in the exit side. Having tested the membranes for gas tightness, tests were conducted to measure H₂ permeability. Prior to the test, the inlet side was vacuumed with a turbomolecular pump. Then the membranes were heated up to 310 °C with 5 °C /min. and enough time was given for temperature stabilization. The high purity H₂ gas was fed to the inlet, initially at 1 bar which was then increased to 10 bar with an increment of 0.5 bar.

A large number of samples were prepared with various thin film compositions. Unfortunately many of these samples were cracked when they were first loaded with H₂. Only a few could withstand when they were first loaded with hydrogen. However, these membranes were also suddenly failed during heating/testing.

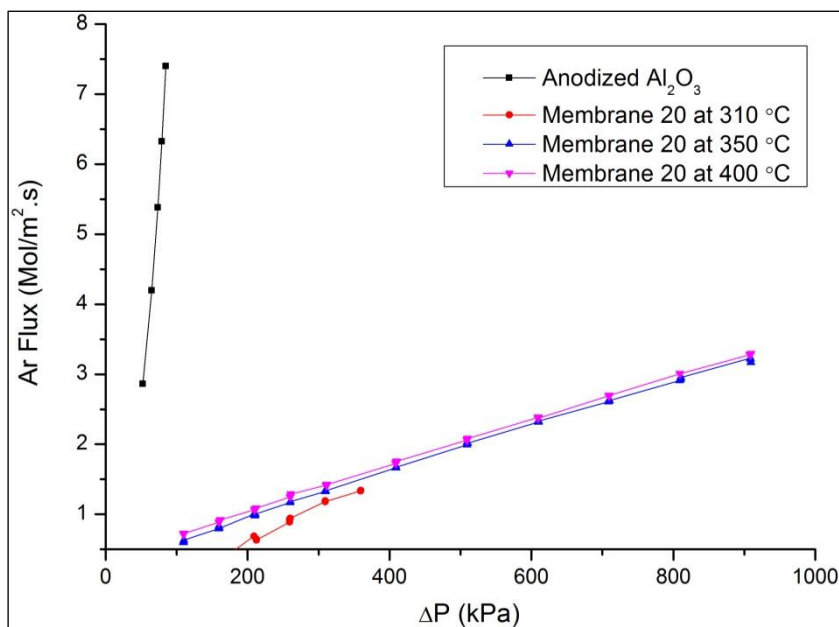


Figure 4.15. H₂ flux versus pressure difference curves of Membrane 20 at various test temperatures.

Of the membranes tested, a sample which could come close to a successful measurement refers to Membrane 20 (close to Pd corner in the sample triangle). Hydrogen flux versus pressure difference for this membrane is included in Figure 4.15. The same plot against square root of pressure difference at 310, 350 and 400 °C are shown plotted in Figure 4.16. The relationship here is not linear. But fitting a straight line to these data yields permeance values of 2.79×10^{-2} , 2.33×10^{-2} , and 2.39×10^{-2} mol/m².s.Pa^{1/2} for 310, 350 and 400 °C respectively. Since films were 3 micron thick this yields a permeability value of 8.37×10^{-8} , 6.99×10^{-8} and 7.17×10^{-8} mol/m².s.Pa^{1/2} in the respective order.

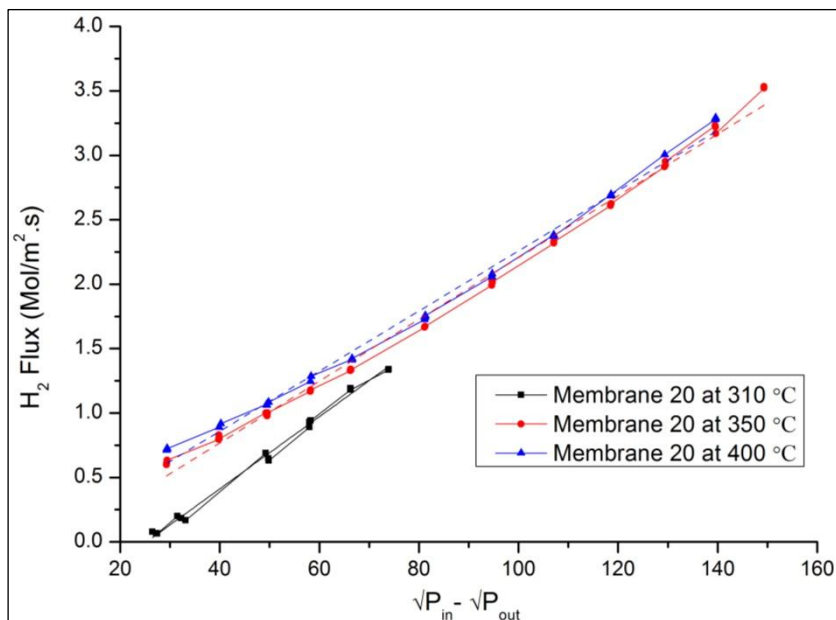


Figure 4.16. H₂ flux versus square root of pressure difference curves of Membrane 20 at various test temperatures.

Permeability values reported in the literature for pure Pd are $1.0\text{-}2.0 \times 10^{-8}$ (Ryi *et al.* 2006). The values reported above are almost an order of magnitude larger. To check the reliability of the permeability values further, activation energy was calculated using equation 2.5. Plot of $\ln(k)$ versus $1/T$ is given in Figure 4.17. It is seen that the relationship is not linear. Here the line is expected to have a negative slope so the third point at $T = 310$ °C ($1/T = 1.71 \times 10^{-3}$ K⁻¹) is totally out of range. Ignoring the data at 310 °C, the activation energy has a value of 1.77 kJ/mol. This is very low as compared to values reported in the literature ($\approx 11\text{-}12$ kJ/mol Weyten *et al.* 2000, 11 kJ/mol Amandusson *et al.* 2001 and 135.5 kJ/mol Ryi *et al.* 2006).

Flux versus difference in pressure (or square root of pressure difference) relationship is probably the result of two parallel processes; one is the permeation of hydrogen through the deposited membrane and the other flow of hydrogen gas through pores existing in the membranes.

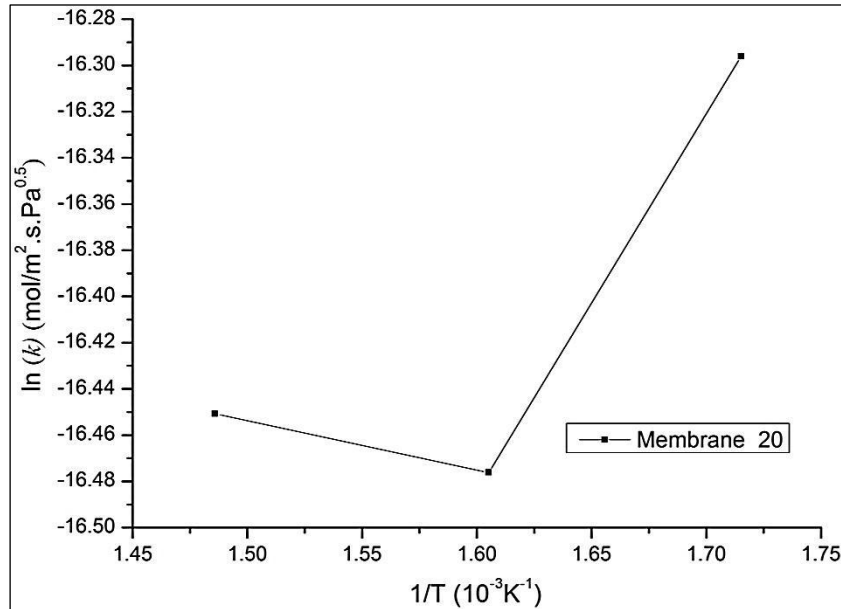


Figure 4.17. Logarithm of hydrogen permeability versus the inverse of test temperature for Membrane 20. The test temperatures are 310, 350 and 400 °C.

4.4. Discussion

In the current study, the aim was to develop of a thin film deposition system that will allow for compositional variation. The system manufactured had three sputter targets suitable positioned so that it was possible to deposit a total 21 sample each 19 mm diameter. The sputter deposition was capable of yielding films that were homogenous in their thickness $\pm 7\%$. EDS analysis of the films deposited in Pd-Nb-Ti have shown that the compositional variations obtained in the film cover a greater portion of the ternary phase diagram.

Sputter deposition carried out in different conditions showed that it was possible to control the microstructure of the deposited films. Films deposited with high pressure of plasma gas (Ar, 10 mTorr) and without substrate heating lead to amorphous/nanocrystalline films, whereas films deposited with low pressure plasma gas (Ar, 5 mTorr) with substrate heating tend to produce crystalline films.

Thus, the thin film deposition system would allow membranes of various chemical compositions in different physical state to be deposited so as to identify membranes (composition and structure) best suited for hydrogen separation.

Another aim of the current study was to develop a permeability tester suitable for thin film membranes. The tester as manufactured would allow testing of membranes up to 10 bar of hydrogen and the temperature could be as high as 450 °C. Furthermore, the tester would allow very low flow rates 0-10 sccm to be measured with high sensitivity while the greater flow rates are measured with a different flow rate controller/meter.

With the use of the current deposition and the permeability tester, it is possible to scan through the deposited samples so as to identify compositions that would have favorable permeation characteristics.

A major difficulty in the current work occurred with regard to materials that need to be used to support the thin film membranes. Both TiO₂ modified PSS and AAO were inadequate in this respect.

TiO₂ modified PSS when used as a substrate, films deposited at 300 °C had a typical Zone-I structure. This is an island growth structure which is often the case for metallic films deposited on insulator substrates. The characteristic of this type of deposition is that they typically have tapered crystallites with domed tops that are separated from one another by open voids. Thus the deposited films with such structure are not expected to be pore free as was verified in the current work. All such deposited membranes were not leak tight even when tested with argon at room temperature (It should be mentioned that this lack of leak tightness might be due to the accidental presence of a relatively large pore in the support material rather than the voids in the deposited film).

Another aspect that can influence the structure of the thin films which is relevant to TiO₂ modified PSS may be the surface roughness of the substrate. Since the rough substrate surfaces with various defects can provide preferred nucleation sites, this may lead to shadowing effects in further deposition of atoms onto the surface. Similarly, the oblique deposition which is the case in the current study, may also lead to shadowing effect which is especially important for the low temperature, Zone-1, depositions. This would yield more open structures in the thin film. The reason is the insufficient mobility of the atoms in the case of low temperature to fill the voids in the structure via surface diffusion.

As an alternative substrate material anodic porous alumina possesses superior properties. Pore structure in AAO is very regular where the probability of accidental presence of large pores is extremely low. Films deposited on AAO were gas tight when tested with Ar. This implies that with the smooth AAO surface the deposition probably leads to films which are pore free. AAO on the other hand is extremely fragile and difficult to handle with pressure and temperature conditions involved in the permeability measurements.

Similar problems were faced in the literature. Thus, as reviewed in section 2.2.1, most studies report permeability values together with values for the selectivity. Since the dense metallic membranes exhibit infinite hydrogen selectivity, lower values reported in the literature imply that the membranes were not defect free. The selectivity reported for such membranes have values of e.g. 24 (Li *et al.* 1993), 1500 (Tong *et al.* 2005) and 5000 (Mardilovich *et al.* 1998) etc. In this respect, the study by Ryi *et al.* 2006 is quite exceptional in that they obtained infinite selectivity in a 4 µm thick membranes. They achieved this selectivity in Pd-Cu-Ni only in the case of the post heat treatment termed as copper re-flow technique. They annealed the membrane at 650 °C where a copper rich phase re-melted and flowed to fill the defects in the structure.

An alternative to re-flow technique could be the deposition of thicker films as proposed by Xiong *et al.* 2010. In this study, ternary system of Nb-Ti-Ni membranes was produced via sputter depositions to different thicknesses up to 12 µm. They found that a minimum thickness of 6 µm was required to obtain gas tight membranes. This study indicates that the deposition of thicker films can be a solution to produce thin film membranes that are gas-tight.

The main purpose of this study is to search through compositions rapidly and effectively so as to identify membrane compositions with highest permeability. The presence of defects or pores in the deposited films creates difficulty since this would make the permeability measurement rather difficult. This was indeed the case in the current study. An approach would be to tolerate the presence of defects but still to measure the permeability within acceptable limits, i.e. to measure it such a manner that the identification of favorable compositions are possible. An approach to do this would be to use a metallic support material with as high permeability as possible.

As reviewed in section 2.2.1.2 b.c.c. metals Nb, V and Ta has the highest permeability among the known metallic materials. Of these, Nb with the permeability of 1.6×10^{-6} (500 °C) has the highest value. Nb can be produced in foil form and when used as a support material can allow the deposition of dense thin film membranes or even in the case of membrane which are not fully dense, it acts as a backup layer which reduces the contribution of defects to the total flux so that measured permeability is representative of the membrane composition.

CHAPTER 5

CONCLUSIONS AND RECOMMENDATION FOR FUTURE WORK

The current study deals with hydrogen separation membranes and aims to develop infrastructure for rapid identification of membrane compositions with the highest permeability. The study was made up of three parts. a) development of sputter deposition system that would allow compositional variation, b) development of substrate material that would support the thin film membranes and would allow permeability measurement and c) development of a set-up to measure the permeability of the thin film membranes. The followings can be concluded from the current study;

- i) A sputter deposition system incorporating three sputter targets were successfully constructed. The vacuum chamber of 450 mm diameter and 400 mm height, which would allow substrates of up to ≈ 150 mm diameter to be deposited. The system as tested with Pd-Nb-Ti after necessary adjustment would yield thin film of homogenous thickness ($\leq 7\%$).
- ii) A total 21 substrates each 19 mm diameter arranged in triangular form in the substrate holder could successfully be deposited where the composition distributions covered a greater portion of Pd-Nb-Ti ternary phase diagram.
- iii) The structure of the deposited thin films can successfully be controlled by substrate temperature as well as by the pressure of plasma gas (Ar). With the help of these parameters, structural diversity also can be produced beside the compositional variety.

As for support material, two options were evaluated which showed that;

- iv) TiO₂ modified porous stainless steel is suitable as support material but due to its associated surface roughness leads to the deposition of films with a defect structure which as a result is not gas tight.
- v) Anodic porous alumina (AAO) is also suitable as a support material as it has a regular pore structure. However, even though its surface with regular 40-60 nm pores provides a suitable surface for thin film depositions, AAO is very delicate and fragile which makes it difficult to adapt it for permeability measurement/hydrogen separation purposes.

For permeability testing;

- vi) A set-up was developed which is capable of measurement over a wide pressure and temperature conditions. The set-up allows hydrogen pressures up to 10 bar and temperature of testing could be as high as 450 °C.

It is recommended that so as to identify compositions with improved permeability, Nb or a similar material which has extremely high permeability could be used as a support material. This would tolerate the evaluation of the films which are not totally defect free.

REFERENCES

- Adhikari S. and Fernando S., "Hydrogen Membrane Separation Techniques", *Industrial & Engineering Chemistry Research*, 45, 875-881, 2006
- Altinisik O., Dogan M., Dogu G., "Preparation and characterization of palladium-plated porous glass for hydrogen enrichment", *Catalysis Today*, 105, 641-646, 2005
- Amandusson H., Ekedahl L.G., Dannetun H., "Hydrogen permeation through surface modified Pd and PdAg membranes", *Journal of Membrane Science*, 193, 35-47, 2001
- Anderson G.S., Mayer W.N., Wehner G.K., *Journal of Applied Physics*, 33, 2291, 1962
- Athayde A.L., Baker R.W., Nguyen P., "Metal Composite membranes for hydrogen separation", *Journal of Membrane Science*, 94, 299-311, 1994
- Awakura Y., Nambu T., Matsumoto Y., Yukawa H., "Hydrogen solubility and permeability of Nb-W-Mo alloy membrane", *Journal of Alloys and Compounds*, 509, 877-880, 2011
- Basile A. and Gallucci F., "A Review of Membrane Reactors", *Membranes for Membrane Reactors: Preparation, Optimization and Selection*, 2011
- Bernardo P., Drioli E., Golemme G., "Membrane Gas Separation: A Review/State of the Art", *Industrial & Engineering Chemistry Research*, 48, 4638-4663, 2009
- Boerrigter H. and Rauch R., "Review of applications of gases from biomass gasification", *Handbook Biomass Gasification*, 2005
- Brodowsky H. and Poeschel E., *Zeitschrift Fur Physikalische Chemie*, 44, 143, 1965
- Bryden K.J. and Ying J.Y., "Nanostructured palladium membrane synthesis by magnetron sputtering", *Materials Science and Engineering*, 204, 140-145, 1995
- Bryden K.J., Ying J.Y., "Nanostructured palladium-iron membranes for hydrogen separation and membrane hydrogenation reactions", *Journal of Membrane Science*, 203, 29-42, 2002
- Buxbaum R.E. and Kinney A.B., "Hydrogen Transport through Tubular Membranes of Palladium-Coated Tantalum and Niobium", *Industrial & Engineering Chemistry Research*, 35, 1996
- Chen S.C., Tu G.C., Hung C.C.Y., Huang C.A., Rei M.H., "Preparation of palladium membrane by electroplating on AISI 316L porous stainless steel supports and its use for methanol steam reformer", *Journal of Membrane Science*, 314, 5-14, 2008
- Cheng Y.S., Yeung K.L., "Palladium-silver composite membranes by electroless plating technique", *Journal of Membrane Science*, 158, 127-141, 1999
- Cortes C.G., Tzimas E., Peteves S.D., "Technologies for Coal based Hydrogen and Electricity Co-production Power Plants with CO₂ Capture", *JRC Scientific and Technical Reports*, 2009

- Dąbrowski A., "Adsorption-from Theory to Practice", *Advances in Colloid and Interface Science*, 93, 135-224, 2001
- Dobkin D.M. and Zuraw M.K., "Principles of Chemical Vapor Deposition", Kluwer Academic Publishers, 2003
- Dolan M., Dave N., Morpeth L., Donelson R., Liang D., Kellam M., Song S., "Ni-based amorphous alloy membranes for hydrogen separation at 400 °C", *Journal of Membrane Science*, 326, 549-555, 2009
- Dolan M.D., Song G., Liang D., Kellam M.E., Chandra D., Lamb J.H., "Hydrogen transport through V85Ni10M5 alloy membranes", *Journal of Membrane Science*, 373, 14-19, 2011
- Evard E.A., Kurdumov A.A., Berseneva F.N., Gabis I.E., "Permeation of hydrogen through amorphous ferrum membrane", *International Journal of Hydrogen Energy*, 26, 457-460, 2001
- Ferrari M. and L. Lutterotti, "Method for the simultaneous determination of anisotropic residual stresses and texture by X-ray diffraction", *Journal of Applied Physics*, 76, 7246-55, 1994
- Fort D., Farr J.P.G., Harris I.R., "A comparison of palladium-silver and palladium-yttrium alloys as hydrogen separation membranes", *Journal of the Less Common Metals*, 39, 293-308, 1975
- Gao H.Y., Lin Y.S., Li Y.D., Zhang B.Q., "Chemical Stability and Its Improvement of Palladium-Based Metallic Membranes", *Industrial & Engineering Chemistry Research*, 43, 6920-6930, 2004
- Gapontsev, A.V., Kondrat'ev V.V., "Hydrogen diffusion in disordered metals and alloys", *Physics-Uspekhi*, 46, 1077-1098, 2003
- Gillespie L.J., Galstaun L.S., "The Palladium-Hydrogen Equilibrium and New Palladium Hydrides", *Journal of the American Chemical Society*, 58, 2565-2573, 1936
- Graham T., "On the absorption and dialytic separation of gases by colloid septa", *Philosophical Transactions of the Royal Society*, 156, 399, 1866
- Gryaznov V., "Metal Containing Membranes for the Production of Ultrapure Hydrogen and the Recovery of Hydrogen Isotopes", *Separation & Purification Reviews*, 29, 171-187, 2000
- Hashi K., Ishikawa K., Matsuda T., Aoki K., "Microstructure and hydrogen permeability in Nb-Ti-Co multiphase alloys", *Journal of Alloys and Compounds*, 425, 284-290, 2006
- Hashi K., Ishikawa K., Matsuda T., Aoki K., "Microstructures and Hydrogen Permeability of Nb-Ti-Ni Alloys with High Resistance to Hydrogen Embrittlement", *Materials Transactions*, 46, 1026-1031, 2005
- Hill E.F., "Hydrogen Separation Using Coated Titanium Alloys", US Patent 4,468,235, 1984
- Hinchcliffe, A.B. and Porter, K.E., "A comparison of membrane separation and distillation", *Transactions of the Institution of Chemical Engineers*, 78, 255, 2000
- Holladay J.D., Hu J., King D.L., Wang Y., "An Overview of Hydrogen Production Technologies", *Catalysis Today*, 139, 244-260, 2009

- Holleck G.L., "Diffusion and solubility of hydrogen in palladium and palladium--silver alloys", *Journal of Physical Chemistry*, 74, 503-511, 1970
- Howard B.H., Killmeyer R.P., Rothenberger K.S., Cugini A.V., Morreale B.D., Enick R.M., Bustamante F., "Hydrogen permeance of palladium-copper alloy membranes over a wide range of temperatures and pressures", *Journal of Membrane Science*, 241, 207-218, 2004
- Huang L., Chen C.S., He Z.D., Peng D.K., Meng G.Y., "Palladium membranes supported on porous ceramics prepared by chemical vapor deposition", *Thin Solid Films*, 302, 98-101, 1997
- Hunter J.B., "A New Hydrogen Purification Process", *Platinum Metals Review*, 4, 130-131, 1960
- Hurlbert R.C., Konecny C.H., "Diffusion of hydrogen through palladium", *Journal of Chemical Physics*, 34, 655, 1961
- Itoh N., Akiha T., Sato T., "Preparation of thin palladium composite membrane tube by a CVD technique and its hydrogen permselectivity", *Catalysis Today*, 104, 231-237, 2005
- Jayaraman V. and Lin Y.S., "Synthesis and Hydrogen Permeation Properties of Ultrathin Palladium-Silver Alloy Membranes", *Journal of Membrane Science*, 104, 251-262, 1995
- Jayaraman V., Lin Y.S., Pakala M., Lin R.Y., "Fabrication of ultrathin metallic membranes on ceramic supports by sputter deposition", *Journal of Membrane Science*, 99, 89-100, 1995
- Jun C.S. and Lee K.H., "Palladium and palladium alloy composite membranes prepared by metal-organic vapor deposition method (cold-wall)", *Journal of Membrane Science*, 176, 121-130, 2000
- Kalinci, Y., Hepbasli A., Dincer I., "Biomass-Based Hydrogen Production: A Review and Analysis", *International Journal of Hydrogen Energy*, 34, 8799-8817, 2009
- Kamakoti P. and Sholl D.S., "A comparison of hydrogen diffusivities in Pd and CuPd alloys using density functional theory", *Journal of Membrane Science*, 225, 145-154, 2003
- Kapoor A., Yang R. T., Wong C., "Surface diffusion", *Catalysis Reviews*, 31, 129-214, 1989
- Karpova R.A. and Tverdovskii I.P., *Journal of Scientific Instruments*, 33, 615, 1959
- Keltte H. and Bredesen R., *Membrane Technology*, 75, 7, 2005
- Kim D.W., Park Y.J., Moon J.W., Ryi S.K., Park J.S., "The effect of Cu reflow on the Pd-Cu-Ni ternary alloy membrane fabrication for infinite hydrogen separation", *Thin Solid Films*, 516, 3036-3044, 2008
- Kirk-Othmer, *Encyclopedia of Chemical Technology*, Wiley-Interscience, 2004
- Knapton A.G., "Palladium alloys for hydrogen diffusion membranes - A review of high permeability materials", *Platinum Metals Review*, 21, 44-50, 1977
- Kong J., Shen H., Chen B., Li Z., Shi W., Yao W., Qi Z., "The abnormal structure of nanocrystalline titanium films prepared by d.c. sputtering", *Thin Solid Films*, 207, 51-53, 1992
- Kruger F. and Gehm G., *Annln. Phys.*, 16, 190, 1933

- Kuraoka K., Zhao H., Yazawa T., "Pore-filled palladium-glass composite membranes for hydrogen separation by novel electroless plating technique", *Journal of Materials Science Letters*, 39, 1879-1881, 2004
- Lee D.W., Lee Y.G., Nam S. E., Ihm S.K., Lee K.H., "Study on the variation of morphology and separation behavior of the stainless steel supported membranes at high temperature", *Journal of Membrane Science*, 220, 137-153, 2003
- Lee W. N., Hwang S. T., "Transport of condensable vapors through a microporous Vycor glass membrane", *Journal of Colloid and Interface Science*, 110, 544-555, 1986
- Lewis F.A., "The Palladium Hydrogen System", Academic Press, 1967
- Li Z.Y., Maeda H., Kusakabe K., Morook S., Anzai H., Akiyama S., "Preparation of palladium-silver alloy membranes for hydrogen separation by the spray pyrolysis method", *Journal of Membrane Science*, 78, 247-254, 1993
- Liu B.S., Zhang W.D., Dai W.L., Deng J.F., "Thermal stability, hydrogen adsorption and separation performance of Ni-based amorphous alloy membranes", *Journal of Membrane Science*, 244, 243-249, 2004
- Liu Y., Subramanian D., Ritter J. A., "Theory and Application of Pressure Swing Adsorption for the Environment in Adsorption and Its Application in Industry and Environmental Protection", Elsevier, 1999
- Luo W., Ishikawa K., Aoki K., "Highly hydrogen permeable NbTiCo hypereutectic alloys containing much primary bcc-(Nb, Ti) phase", *International journal of hydrogen energy*, 37, 2793-2797, 2012
- Magnone E., Jeon S.I., Park J.H., E. Fleury, "Hydrogen Permeation Properties and Chemical Stability of Novel Pd-Free Alloy Membranes Based on the V-Y System", *Chemical Engineering & Technology*, 35, 469-472, 2012
- Makceehan L.W., "The crystal structures of the system palladium-hydrogen", *Physical Review*, 21, 334, 1923
- Makrides A.C., "Absorption of Hydrogen by Silver-Palladium Alloys", *Journal of Physical Chemistry*, 68, 2160-2169, 1964
- Mardilovich I.P., Engwall E.E., Ma Y.H., "Dependence on the pore size and the plating surface topology of asymmetric Pd-porous stainless steel membranes", *Desalination*, 144, 85-89, 2002
- Mardilovich P.P., She Y., Ma Y.H., Rei M., "Defect free palladium membranes on porous stainless steel support", *AIChE Journal*, 44, 310-322, 1998
- Martin P.M., "Handbook of Deposition Technologies for Films and Coatings", Elsevier, 2002
- Masuda H., Fukuda K., "Ordered metal nanohole arrays made by a two-step replication of honeycomb structures of anodic alumina", *Science*, 268, 1466-1468, 1995
- McCool B. and Lin Y.S., "Nanostructured thin palladium-silver membranes: Effects of grain size on gas permeation properties", *Journal of Materials Science*, 36, 3221-3227, 2001

- McCool B., Xomeritakis G., Lin Y.S., "Composition control and hydrogen permeation characteristics of sputter deposited palladium-silver membranes", *Journal of Membrane Science*, 161, 67-76, 1999
- McKinley D.L., US patent 3,350,845, 1967
- McKinley D.L., US patent 3,439,474, 1969
- Mejdell A.L., Jondahl M., Peters T.A., Bredeesen R., Venvik H.J., "Experimental investigation of a microchannel membrane configuration with a 1.4 μm Pd/Ag23 wt.% membrane-Effects of flow and pressure", *Journal of Membrane Science*, 327, 6-10, 2009
- Miller G.Q. and Stocker, J., "Selection of a Hydrogen Separation Process", National Petrochemical and Refiners Association, 1989
- Molburg, J.C. and Doctor, R.D., 20th Annual International Pittsburg Coal Conference, 2003
- Mooney J.B. and Radding S.B., "Spray Pyrolysis Processing", *Annual Review of Materials Science*, 12, 81-101, 1982
- Morreale B.D., Ciocco M.V., Howard B.H., Killmeyer R.P., Cugini A.V., Enick R.M., "Effect of hydrogen-sulfide on the hydrogen permeance of palladium-copper alloys at elevated temperatures", *Journal of Membrane Science*, 241, 219-224, 2004
- Moss T.S., Peachey N.M., Snow R.C., Dye R.C., "Multilayer metal membranes for hydrogen separation", *International Journal of Hydrogen Energy*, 23, 99-106, 1998
- Movchan B.A. and Demchishin A.V., *Physics of Metals and Metallography*, 28, 653-660, 1969
- Nam S.E. and Lee K.H., "Hydrogen separation by Pd alloy composite membranes: introduction of diffusion barrier", *Journal of Membrane Science*, 192, 177, 2001
- Nam S.E. and Lee K.H., "A study on the palladium/nickel composite membrane by vacuum electrodeposition", *Journal of Membrane Science*, 170, 91-99, 2000
- Nam S.E., Lee S.H., Lee K.H., "Preparation of palladium alloy composite membrane supported in a porous stainless steel by vacuum electrodeposition", *Journal of Membrane Science*, 153, 163-173, 1999
- Nambu T., Shimizu K., Matsumoto Y., Rong R., Watanabe N., Yukawa H., Morinaga M., Yasuda I., "Enhanced hydrogen embrittlement of Pd-coated niobium metal membrane detected by in situ small punch test under hydrogen permeation", *Journal of Alloys and Compounds*, 446-447, 588-592, 2007
- Nishimura C., Komaki M., Hwang S., Amano M.J., "V-Ni alloy membranes for hydrogen purification", *Journal of Alloys and Compounds*, 330-332, 902-906, 2002
- Nishimura C., Ozaki T., Komaki M., Zhang Y.J., "Hydrogen permeation and transmission electron microscope observations of V-Al alloys", *Journal of Alloys and Compounds*, 356-357, 295-299, 2003
- O'Brien J., Hughes R., Hisek J., "Pd/Ag membranes on porous alumina substrates by unbalanced magnetron sputtering", *Surface and Coatings Technology*, 142-144, 253-259, 2001

- Ockwig N.W. and Nenoff T.M., "Membranes for Hydrogen Separation", *Chemical Reviews*, 107, 4078-4110, 2007
- Pagliari S.N. and Way J.D., "Innovations in Palladium Membrane Research", *Separation and Purification Methods*, 31, 1, 2002
- Pagliari S.N., "Development of Group V Based Metal Membranes for Hydrogen Separation", *AIChE Annual Meeting*, Separation Division, 2008
- Pagliari S.N., Pesiri D., Dye R.C., Venhaus T.J., Chandra D., Tewell C.R., Snow R.C., "Palladium Coated Vanadium Alloy Membranes for Hydrogen Separation", *AIChE Annual Meeting*, 2005
- Pagliari S.N., Wermer J.R., Buxbaum R.E., Ciocco M.V., Howard B.H., Morreale B.D., "Development of membranes for hydrogen separation: Pd coated V-10Pd", *Energy Materials: Materials Science and Engineering for Energy Systems*, 3, 169-176, 2008
- Pizzi D., Worth R., Baschetti M.G., Sarti G.C., Noda K., "Hydrogen permeability of 2.5 μm palladium-silver membranes deposited on ceramic supports", *Journal of Membrane Science*, 325, 446-453, 2008
- Pluym T.C., Kodas T.T., Wang L., Glicksman H.D., "Silver-palladium alloy particle production by spray pyrolysis", *Journal of Materials Research*, 10, 1661-1673, 1995
- Pyle, W., "Hydrogen Purification, Home power", *Solar Hydrogen Chronicles*, 67, 42-49, 1998
- Quicker P., Hollein V., Dittmeyer R., "Catalytic dehydrogenation of hydrocarbons in Pd composite membrane reactors", *Catalysis Today*, 56, 21, 2000
- Romm J., "The Hype about Hydrogen", Island Press, 2005
- Ryi S.K., Park J.S., Kim S.H., S.H. Cho, Kim D.W., Um K.Y. "Characterization of Pd-Cu-Ni ternary alloy membrane prepared by magnetron sputtering and Cu-reflow on porous nickel support for hydrogen separation", *Separation and Purification Technology*, 50, 82-91, 2006
- Ryoo R., Joo S. H., Kruk M., Jaroniec M., "Ordered Mesoporous Carbons", *Advanced Materials*, 13, 677-681, 2001
- Saracco G. and Specchia V., "Catalytic Inorganic-Membrane Reactors: Present Experience and Future Opportunities", *Catalysis Reviews: Science and Engineering*, 36, 305-384, 1994
- Shirasaki Y., Tsuneki T., Ota Y., Yasuda I., Tachibana S., Nakajima H., Kobayashi K., "Development of membrane reformer system for highly efficient hydrogen production from natural gas", *International Journal of Hydrogen Energy*, 34, 4482-4487, 2009
- Steward S.A., "Review of Hydrogen Isotope Permeability through Materials", Lawrence Livermore National Laboratory, 1983
- Su C., Jin T., Kuraoka K., Matsumura Y., Yazawa T., "Thin Palladium Film Supported on SiO₂-Modified Porous Stainless Steel for a High-Hydrogen-Flux Membrane", *Industrial & Engineering Chemistry Research*, 44, 3053-3058, 2005

- Tong H.D., Berg V.A.H.J., Gardeniers J.G.E., Jansen H.V., Gielens F.C., Elwenspoek M.C., "Preparation of palladium-silver alloy films by a dual-sputtering technique and its application in hydrogen separation membrane", *Thin Solid Films*, 479, 89-94, 2005
- Tong J. and Matsumura Y., "Thin Pd membrane prepared on macroporous stainless steel tube filter by an in-situ multi-dimensional plating mechanism", *Chemical Communications*, 21, 2460-2461, 2004
- Tong J., Matsumura Y., Suda H., Haraya K., "Experimental Study of Steam Reforming of Methane in a Thin (6 μm) Pd-Based Membrane Reactor", *Industrial & Engineering Chemistry Research*, 44, 1454-1465, 2005
- Tosti S., Bettinali L., Castelli S., Sarto F., Scaglione S., Violante V., "Sputtered, electroless, and rolled palladium-ceramic membranes", *Journal of Membrane Science*, 196, 241-249, 2002
- Uehara I., "Hydrogen and Natural Gas Mixture", *Energy Carriers and Conversion Systems*, 1, 2002
- Uemiya S., Sato N., Ando H., Kude Y., Matsuda T., Kikuchi E., "Separation of hydrogen through palladium thin film supported on a porous glass tube", *Journal of Membrane Science*, 56, 303-313, 1991
- Ward T.L., Dao T., "Model of hydrogen permeation behavior in palladium membranes.", *Journal of Membrane Science*, 153, 211-231, 1999
- Wasa K. and Hayakawa S., "Handbook of Sputter Deposition Technology", Noyes Publications, 1992
- Weyten H., Luyten J., Keizer K., Willems L., Leysen R., "Membrane performance: the key issues for dehydrogenation reactions in a catalytic membrane reactor", *Catalysis Today*, 56, 3-11, 2000
- Wicke E. and Nernst G., "Phase diagram and thermodynamic behavior of the systems Pd/H₂ and Pd/D₂ at normal temperatures; H/D separation effects", *Berichte der Bunsengesellschaft für physikalische Chemie*, 68, 224, 1964
- Xiong L., Liu S., Rong L., "Fabrication and characterization of Pd/Nb₄₀Ti₃₀Ni₃₀/Pd/porous nickel support composite membrane for hydrogen separation and purification", *International Journal of Hydrogen Energy*, 35, 1643-1649, 2010
- Xomeritakis G. and Lin Y.S., "Fabrication of thin metallic membranes by MOCVD and sputtering", *Journal of Membrane Science*, 133, 217-230, 1997
- Xu J., Froment G.F., "Methane Steam Reforming, Methanation and Water-Gas Shift: I. Intrinsic Kinetics", *AIChE Journal*, 35, 88-96, 1989
- Xue D., Chen H., Wu G.H., Deng J.F., "Amorphous Ni-B alloy membrane: preparation and application in ethanol dehydrogenation", *Applied Catalysis A: General*, 214, 87-94, 2001
- Yamaura S.I., Shimpo Y., Okouchi H., Nishida M., Kajita O., Inoue A., "The Effect of Additional Elements on Hydrogen Permeation Properties of Melt-Spun Ni-Nb-Zr Amorphous Alloys", *Materials Transactions*, 45, 330-333, 2004
- Yeung K.L., Sebastian J.M., Varma A., "Novel preparation of Pd/Vycor composite membranes", *Catalysis Today*, 25, 231-236, 1995

Yukawa H., Nambu T., Matsumoto Y., Watanabe N., Zhang G., Morinaga M., “Alloy Design of Nb-Based Hydrogen Permeable Membrane with Strong Resistance to Hydrogen Embrittlement”, *Materials Transactions*, 49, 2202-2207, 2008

Zander D., Leptien H., Koster U., Eliaz N., Eliezer D.J., “Hydrogenation of Zr-based metallic glasses and quasicrystals”, *Journal of Non-Crystalline Solids*, 252, 893-897, 1999

Zhang K., Gao H., Rui Z., Liu P., Li Y., Lin Y.S., “High-Temperature Stability of Palladium Membranes on Porous Metal Supports with Different Intermediate Layers”, *Industrial & Engineering Chemistry Research*, 48, 1880-1886, 2009

Zhang Y., Ozaki T., Komaki M., Nishimura C., “Hydrogen permeation of Pd-Ag alloy coated V-15Ni composite membrane: effects of overlayer composition”, *Journal of Membrane Science*, 224, 81-91, 2003

Zhang Y., Ozaki T., Komaki M., Nishimura C., “Hydrogen permeation characteristics of vanadium-aluminum alloys”, *Scripta Materialia*, 47, 601-606, 2002